

**AN EXPERIMENTAL EVALUATION
OF THE RADIATION PROTECTION
AFFORDED BY A LARGE MODERN
CONCRETE OFFICE BUILDING**

By

J. F. Batter, Jr., A. L. Kaplan, and E. T. Clarke

Approved by: R. L. CORSBIE

Director

Civil Effects Test Operations

Technical Operations, Inc.

May 1, 1959

ABSTRACT

An experimental study was made to determine the effective shielding provided by a modern reinforced-concrete office building (AEC Headquarters building) from nuclear fallout. Pocket ionization chambers were used for measurement of the radiation-field strength. Fallout was simulated with distributed and point-source configurations of Co^{60} and Ir^{192} sources.

Four typical sections were selected for study, and experiments were performed on each. These included an external wing with exposed basement walls and an external wing with a buried basement. Roof studies were made on an internal wing with a full basement and on the east end of wing A, which has a thin-roof construction. The thick-roof construction of 8 in. of concrete and 2 in. of rigid insulation covers all the building except the east end of wing A, which has 4 in. of concrete and 2 in. of insulation.

ACKNOWLEDGMENTS

The authors wish to express their appreciation to the numerous members of government organizations for their cooperation and support. In particular, we are indebted to:

Members of the Atomic Energy Commission, Division of Biology and Medicine, for the wholehearted cooperation of members of the Civil Effects Test Operations, the Health Protection Branch, and the Radiation Instruments Branch which made this experiment possible.

Members of the General Services Administration for their cooperation in planning experiment locations and providing many support services.

Members of the National Bureau of Standards for suggestions in the planning and analysis of the experiment.

Representatives of the Health Physics Division of the Oak Ridge National Laboratory for their collaboration in planning the experiment.

Finally, the authors are indebted to the Physical Sciences Research Office of the Office of Civil and Defense Mobilization for making available much of the experimental equipment.

CONTENTS

ABSTRACT	5
ACKNOWLEDGMENTS	6
CHAPTER 1 INTRODUCTION	11
1.1 Objectives	11
1.2 Background	11
1.3 Description of AEC Headquarters Building	11
CHAPTER 2 EXPERIMENTAL TECHNIQUES, MATERIALS, AND INSTRUMENTATION	16
2.1 Isotope-handling Equipment	16
2.1.1 Source Circulation System	16
2.1.2 Point-source Handling Equipment	21
2.2 Sources	22
2.3 Source Calibration	22
2.4 Instrumentation	24
2.5 Experimental Technique	24
CHAPTER 3 PRESENTATION OF DATA	30
3.1 Area-source Experiments	30
3.2 Point-source Data	30
CHAPTER 4 ANALYSIS AND CONCLUSIONS	50
4.1 Estimation of Infinite-field Dose	50
4.2 Calculation of Protection Factors	52
4.3 "Near Window" Effect	53
4.4 Effect of Exposed Basement Walls	53
4.5 General Conclusions	59
APPENDIX A RADIATION-SAFETY OPERATIONS	60

ILLUSTRATIONS

CHAPTER 1 INTRODUCTION	
1.1 Wings B and C West of the AEC Headquarters Building	12
1.2 Wing A East of the AEC Headquarters Building	12

ILLUSTRATIONS (Continued)

1.3	Plan View of Building, Illustrating Ground Contours	13
1.4	Sectional View of Building, Illustrating Floor and Wall Thicknesses and Elevations	14
CHAPTER 2 EXPERIMENTAL TECHNIQUES, MATERIALS, AND INSTRUMENTATION		
2.1	Schematic Diagram of Source Circulation System	17
2.2	Isotope Storage Containers	18
2.3	Co ⁶⁰ and Ir ¹⁹² Source Assembly	19
2.4	Co ⁶⁰ Source Assembly	19
2.5	Remotely Located Source Pumping System	20
2.6	Radiographic Unit Used for Point-source Measurements	21
2.7	Cutaway View of the 27-curie Co ⁶⁰ Source Capsule	23
2.8	Calibration Curves for Cobalt and Iridium Sources	23
2.9	PIC Reading Instrument	25
2.10	Mock-up of Remote Radiation Indicating Device	25
2.11	Simulation of a Uniform Rectangular Radiation Field	26
2.12	Simulation of a Semicircular Field of Constant Source Density	26
2.13	Hall Instrumentation, Illustrating Placement of PIC's	27
2.14	Office Instrumentation, Illustrating Placement of PIC's	27
2.15	Experiment Schedule and Locations	28
CHAPTER 3 PRESENTATION OF DATA		
3.1	Location of Area Experiments	32
3.2	Normalized Data for Wing A West	33
3.3	Normalized Data for Wing A East	34
3.4	Normalized Data for Wing B	35
3.5	Normalized Data for Wing C West	36
3.6	Normalized Data for Wing F	37
3.7	Normalized Data for Wing G East	38
3.8	Point Source Below Air Filter in Wing F	39
3.9	Point Source Above Air Filter in Wing F	40
3.10	Point Source Located at Emergency Air Inlet in Wing F	41
3.11	Point Source Below Roof Drain in Wing C	42
3.12	Point Source Below Air Filter in Wing D	43
3.13	Point Source Above Air Filter in Wing D	44
3.14	Point Source Below Roof Drain in Wing D	45
3.15	Point Source in Emergency Air Inlet in Wing D	46
3.16	Point Source Below Air Filter in Wing A	47
3.17	Point Source Above Air Filter in Wing A	48
3.18	Point Source in Emergency Air Inlet in Wing A	49
CHAPTER 4 ANALYSIS AND CONCLUSIONS		
4.1	Diagram of Contaminated Plane with Cleared Circle	51
4.2	Protection Factors from Co ⁶⁰ Radiation in Wing A	54
4.3	Protection Factors from Co ⁶⁰ Radiation in Wing B and Wing C West	55
4.4	Protection Factors from Co ⁶⁰ Radiation in Wing F and Wing G East	56
4.5	Horizontal Dose Distribution on the First Floor from a Semicircular Radiation Field of 280 Ft Radius	57
4.6	Effect of Exposed Basement Wall	58

TABLES

CHAPTER 3 PRESENTATION OF DATA

3.1 Area-source Experiments	31
---------------------------------------	----

CHAPTER 4 ANALYSIS AND CONCLUSIONS

4.1 Data Normalization	53
----------------------------------	----

Chapter 1

INTRODUCTION

1.1 OBJECTIVES

The over-all objective of this project was to determine, for the Atomic Energy Commission, the radiation shielding afforded by its Headquarters building. In addition, the study was concerned with the development of data that would be applicable to general civil defense needs and with a determination of the shielding afforded by a reinforced-concrete structure against a plane source of radiation, including the shielding factor of the roof and floor slabs. The effect of a build-up of radioactive contamination on filters and drain pipes was determined through point-source measurements.

1.2 BACKGROUND

The theory of radiation attenuation in a complex structure is so intricate that computations of shielding must include many approximations and simplifying assumptions to make them operationally useful for national security needs. Beginning in June 1958, full-scale experiments^{1,2} have been performed on residential structures, home shelters of several types, and moderate-size industrial buildings considered typical of older mill and municipal construction to evaluate the inaccuracies introduced by assumptions and simplifications and to provide experimental data useful for both theoretical analysis and practical application.

The AEC has been concerned not only with assisting the national civil defense program but also with the continuity of its operations and, therefore, had a twofold interest in determining the shielding factor of its Headquarters building. Technical Operations, Inc. (TOI), was requested to undertake this study because it had already done some work on large structures for the Office of Civil and Defense Mobilization and had developed a technique for simulating fallout with large (200-curie Co^{60} and up to 400-curie Ir^{192}) sources. The AEC Headquarters building was ideally situated for conducting this study because the building site was sufficiently isolated that use of the relatively high radiation fields did not create any off-site radiation-hazard problems. TOI was responsible, under license to the AEC, for the protection of its personnel; all other radiation-protection aspects of the study and all radiation-safety operations were conducted by AEC employees.

1.3 DESCRIPTION OF AEC HEADQUARTERS BUILDING

The AEC Headquarters building, located 25 miles northwest of Washington, near Germantown, Md., is a modern rambling four-story reinforced-concrete and brick office building. Figures 1.1 and 1.2 are views of wings B and C (west) and wing A (east), which are typical of the construction techniques used. The ground level surrounding this building is approximately even with the first floor in most areas, although several portions of the basement are exposed in varying proportions. Figure 1.3 is a plan view of the building, illustrating its general configurations and the ground-contour levels.

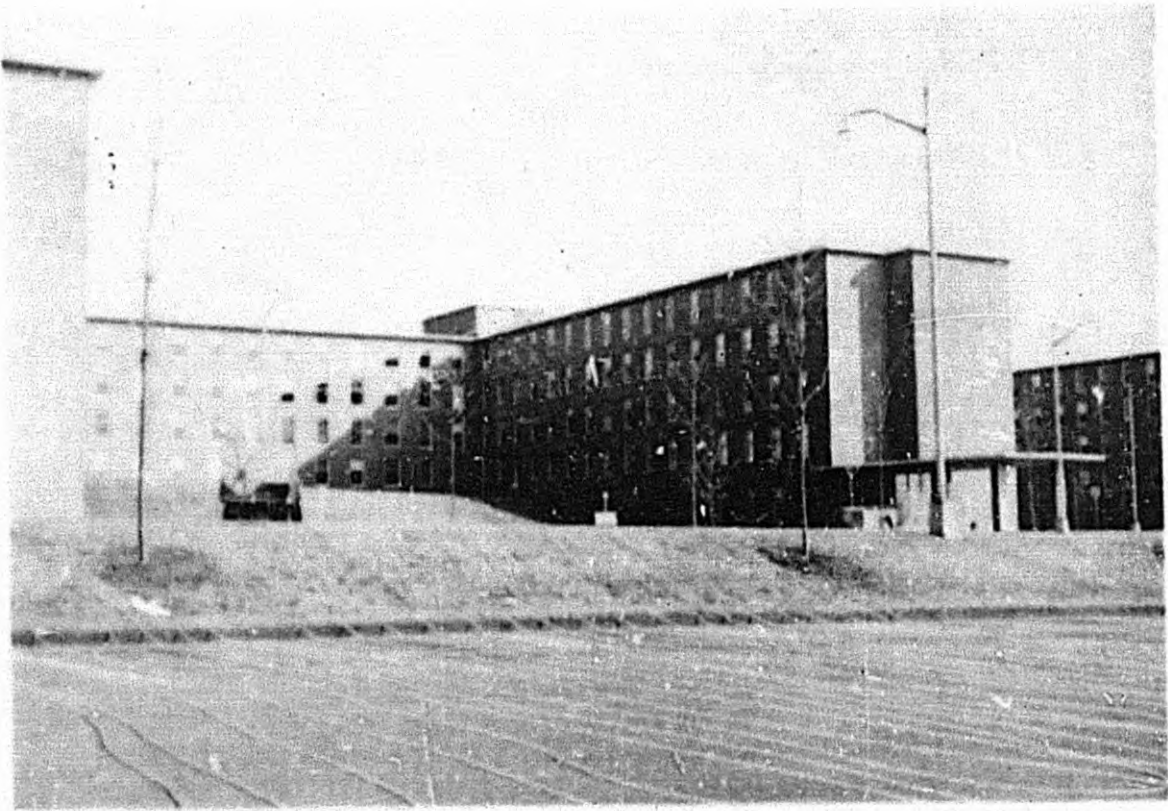


Fig. 1.1 —Wings B and C west of the AEC Headquarters building.

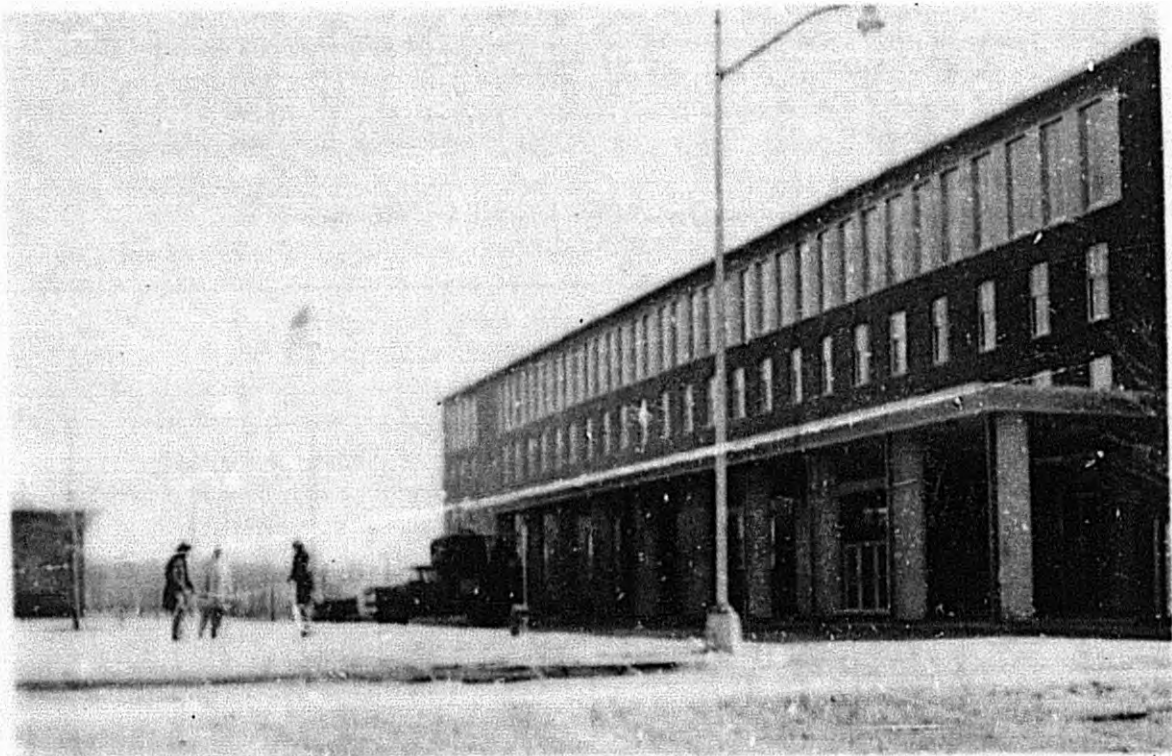


Fig. 1.2 —Wing A east of the AEC Headquarters building.

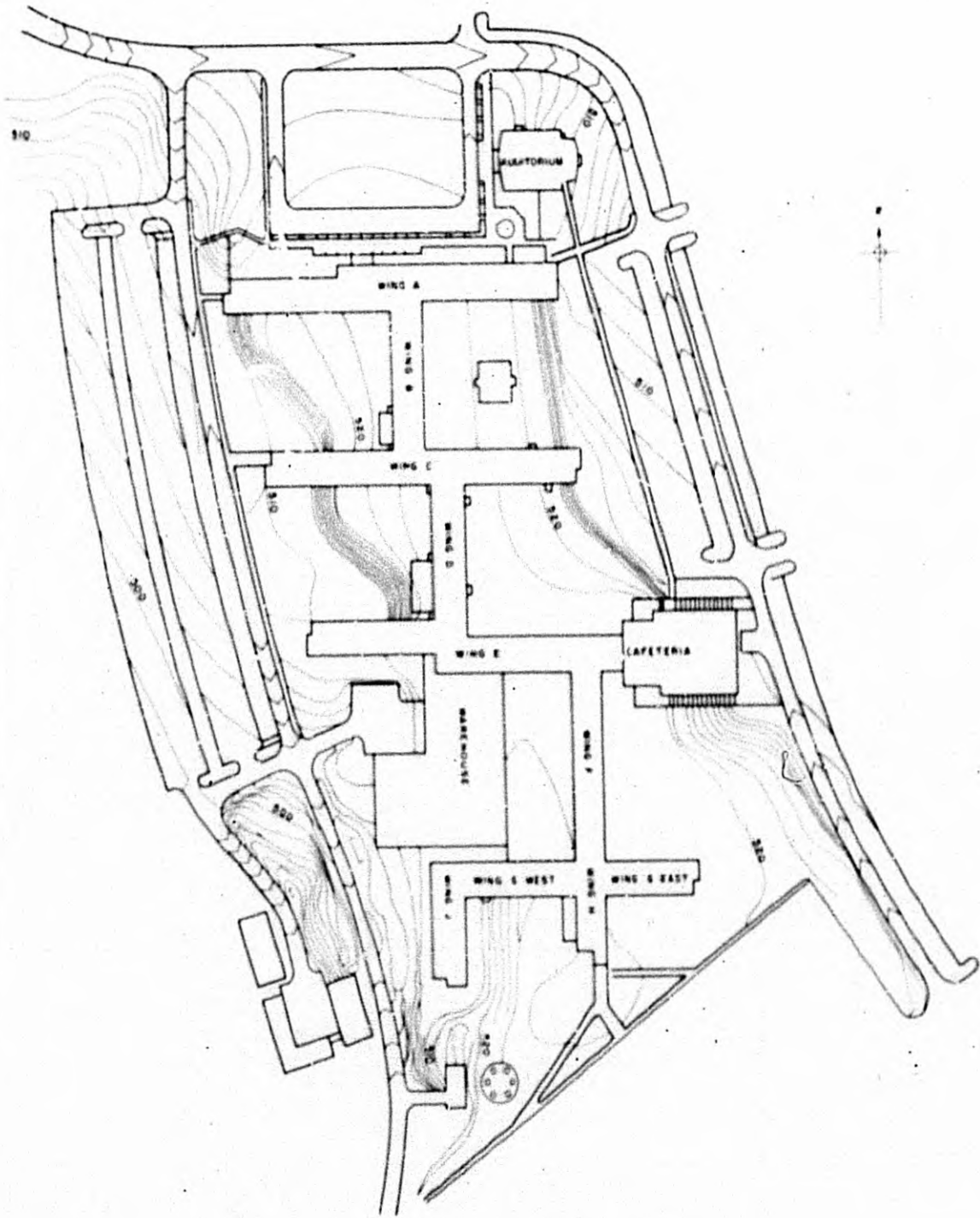


Fig. 1.3 — Plan view of building, illustrating ground contours.

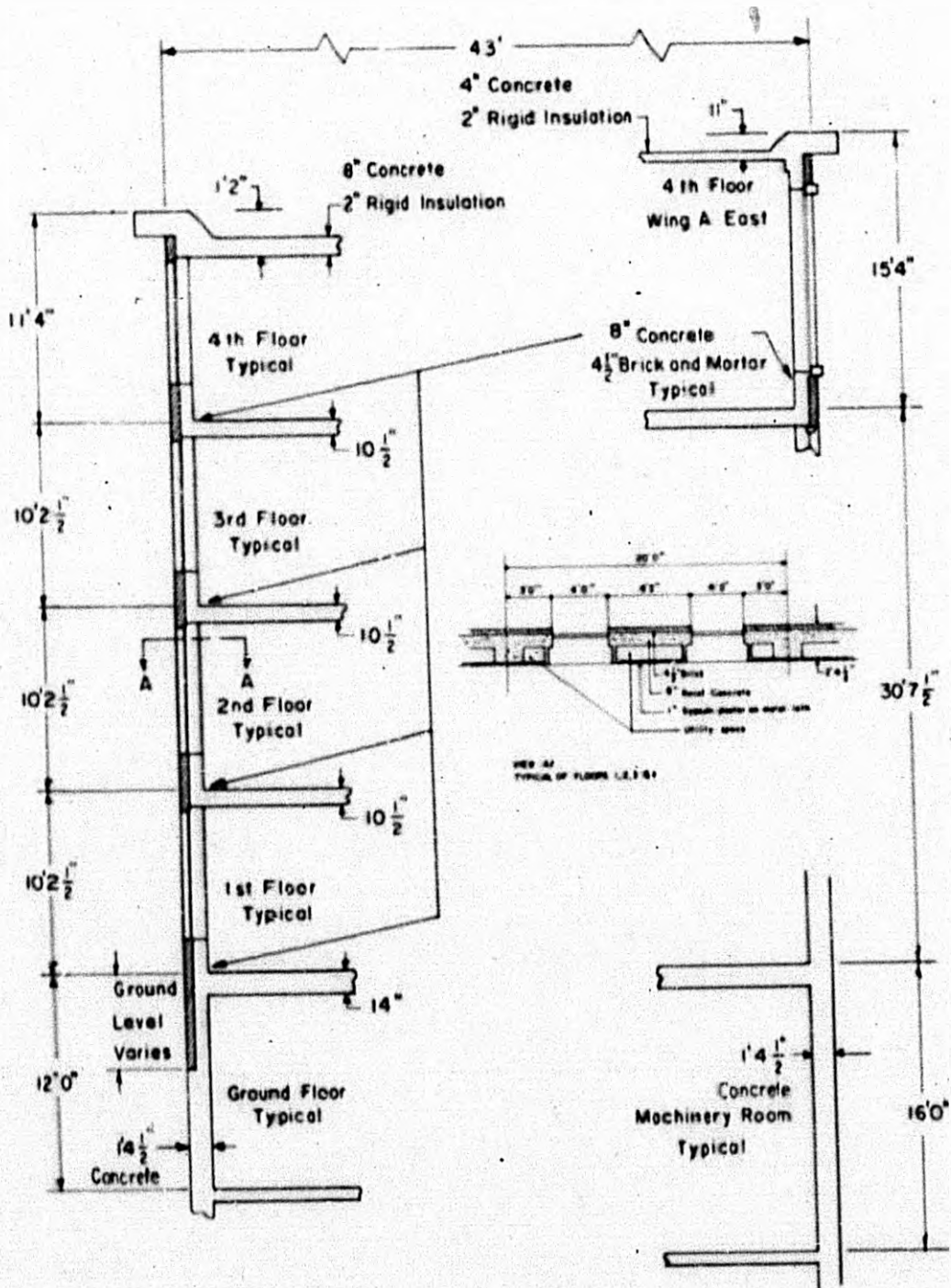


Fig. 1.4—Sectional view of building, illustrating floor and wall thicknesses and elevations.

The building interior walls are constructed of either gypsum block and plaster or removable metal office partitions. Figure 1.4 illustrates the thickness and elevations of the floors and exterior walls. It should be noted that all experiments were performed with the usual complement of office furniture since the building was in normal use throughout the experimentation period.

REFERENCES

1. J. A. Auxier et al., Experimental Evaluation of the Radiation Protection Afforded by Residential Structures Against Distributed Sources, Report CEX-58.1, Jan. 19, 1959.
2. E. T. Clarke et al., Measurement of Attenuation in Existing Structures of Radiation from Simulated Fallout, Report TOB 59.4, Apr. 2, 1959.

Chapter 2

EXPERIMENTAL TECHNIQUES, MATERIALS, AND INSTRUMENTATION

2.1 ISOTOPE-HANDLING EQUIPMENT

Two distinct techniques of isotope handling were employed. One method simulated a plane horizontal radiation field either on the ground or on the roof of the structure, and the other method accurately positioned a source for point-source measurements. With the first method a source was circulated from a storage container through a long prepositioned tube and back into the storage container. The second employed a standard radiographic gamma-ray source projector.

2.1.1 Source Circulation System

For experimental measurement of the protection afforded by a structure against simulated fallout radiation, a special source circulation system has been devised to simulate a uniformly contaminated area. With this system a sealed source is hydraulically pumped at a uniform rate through a long length of polyethylene tubing. This tubing, which can be used in lengths of many thousands of feet, is prepositioned over the area where a radiation field is to be generated. If the amount of tubing per unit area is kept constant, the source will spend a constant amount of time per unit area, thus simulating constant-density fallout when the radiation intensity is time-integrated by isotropic detectors.

Figure 2.1 is a schematic drawing of the source circulation system, showing the four basic components, i.e., the polyethylene tube through which the source is circulated, the pumping system that drives the source through the tube, the isotope storage containers (see Fig. 2.2), and the isotope source capsule (Figs. 2.3 and 2.4).

The pumping system (Fig. 2.5) is comprised of three pumps, two slow-speed constant-volume water pumps for producing constant velocity of the source assembly in the polyethylene tubing and a high-volume gear pump for initial filling of the tube and for moving the source at high speed. The low-speed constant-volume pumps will drive the source assembly at any predetermined rate between 50 and 3000 ft/hr. The high-speed pump permits source assembly velocities up to about 20,000 ft/hr (but not necessarily at a uniform rate) when desired. Hand valves in the pumping system permit initial selection of the desired pump.

The low-speed constant-volume pumps and the high-speed gear pump are connected by means of hand-operated valves to a main high-pressure manifold. This manifold contains a pressure-relief valve set at 100 psi, which dumps the pumping solution (water) back to the main reservoir, and a remotely operated solenoid valve, which can either apply pressure to the rear of the source assembly in the storage pig or return the water to the reservoir. Initially, the solenoid valve is adjusted to bypass the water flow from the pump to the reservoir, and the pump is started. When circulation of the source is desired, the solenoid valve is actuated to connect the output of the pump to the tube leading to the storage pig. The water flow then acts on the source piston, forcing the source (see Figs. 2.3 and 2.4) out into the long length of polyethylene tubing and finally back into the opposite tube of the storage pig.

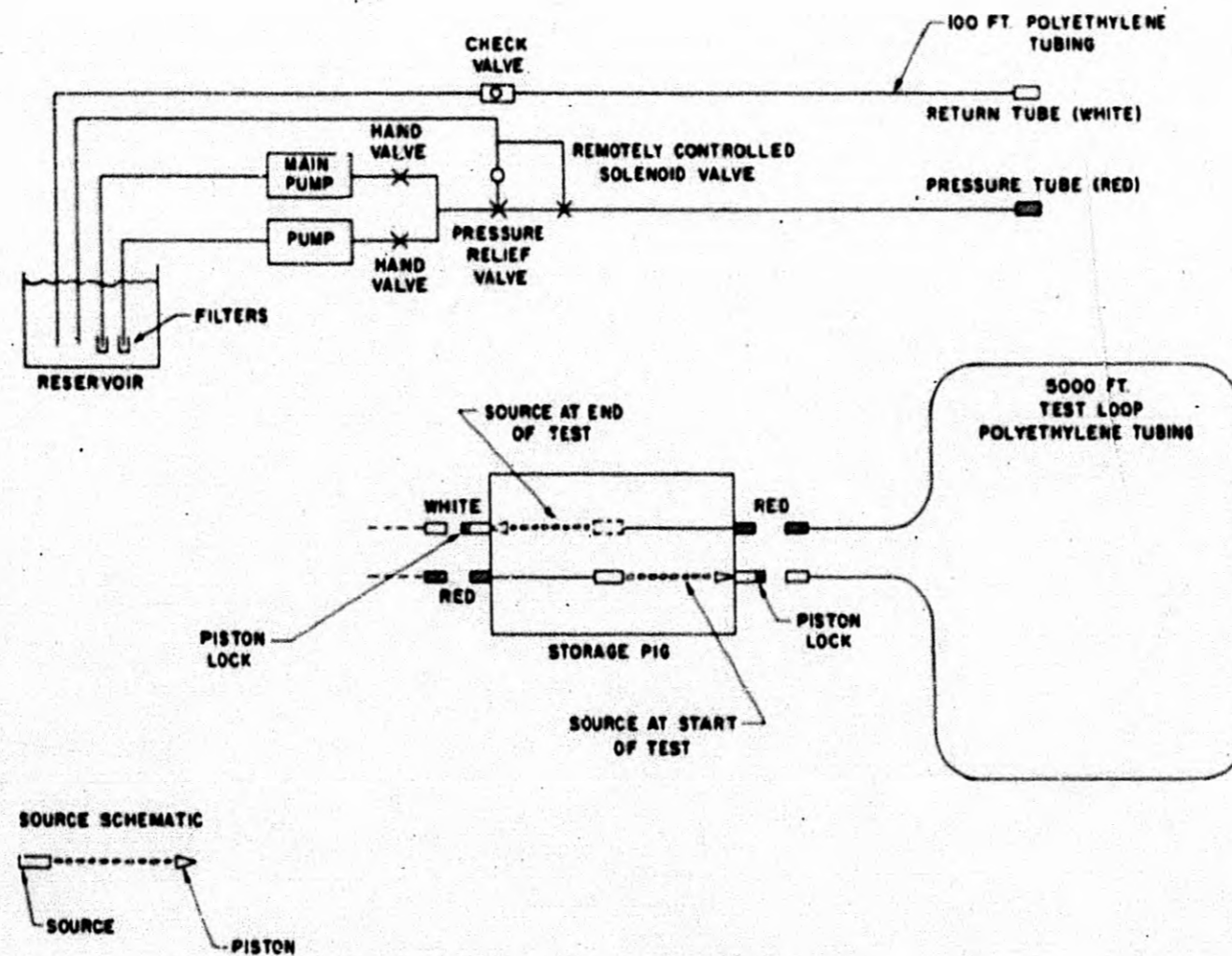
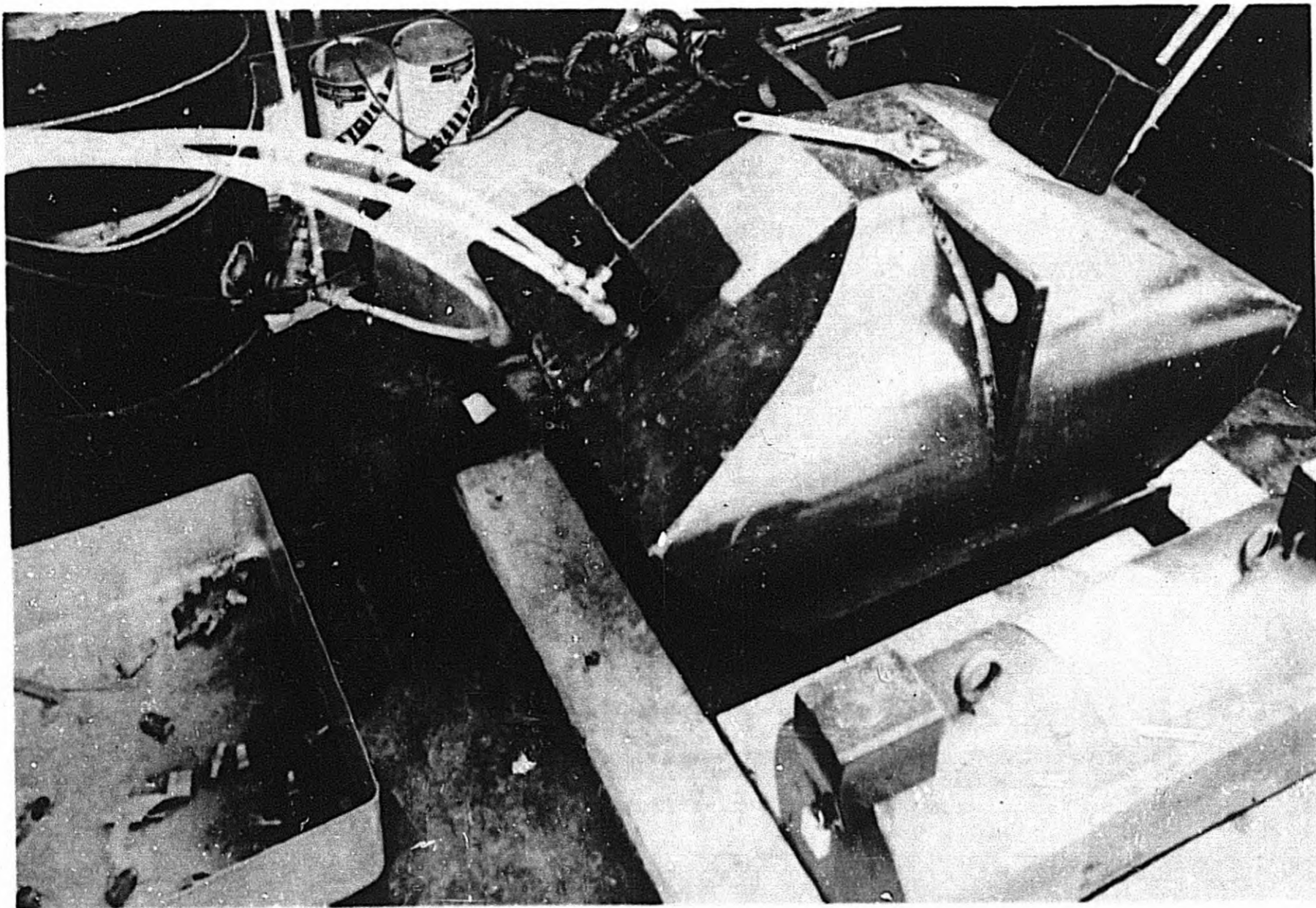


Fig. 2.1 — Schematic diagram of source circulation system.



18

Fig. 2.2—Isotope storage containers.

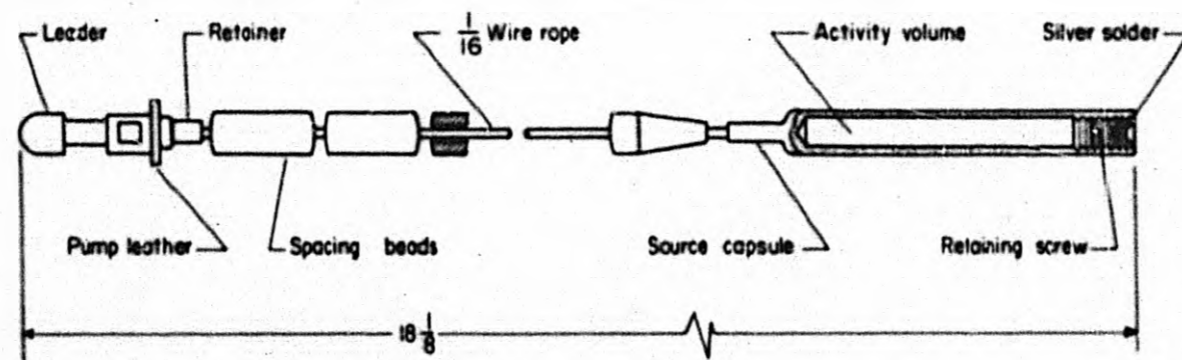


Fig. 2.3— Co^{60} and Ir^{192} source assembly.

19

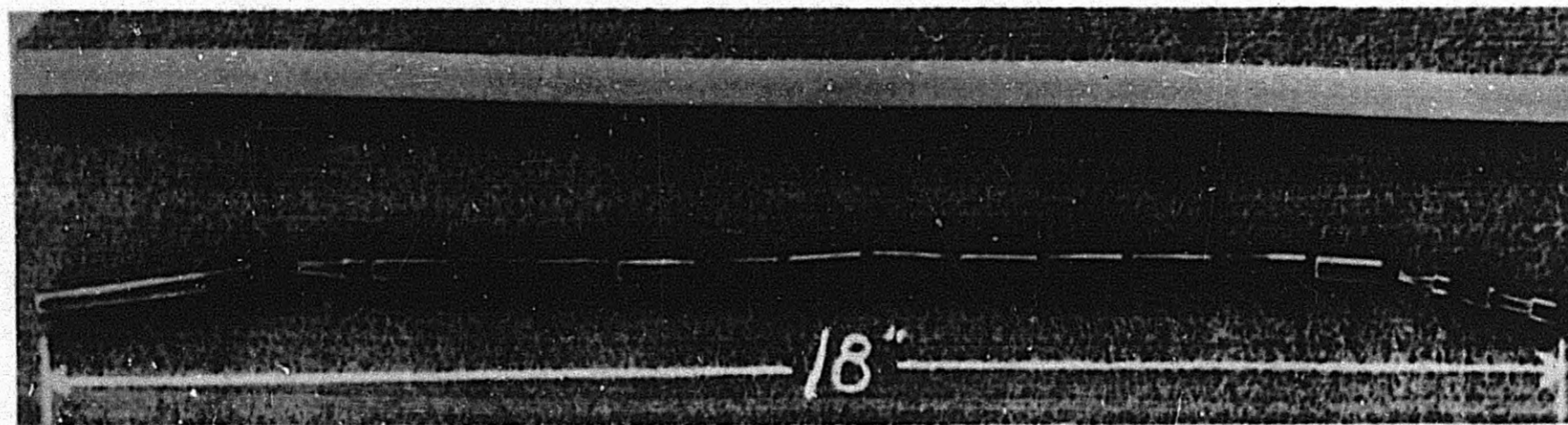
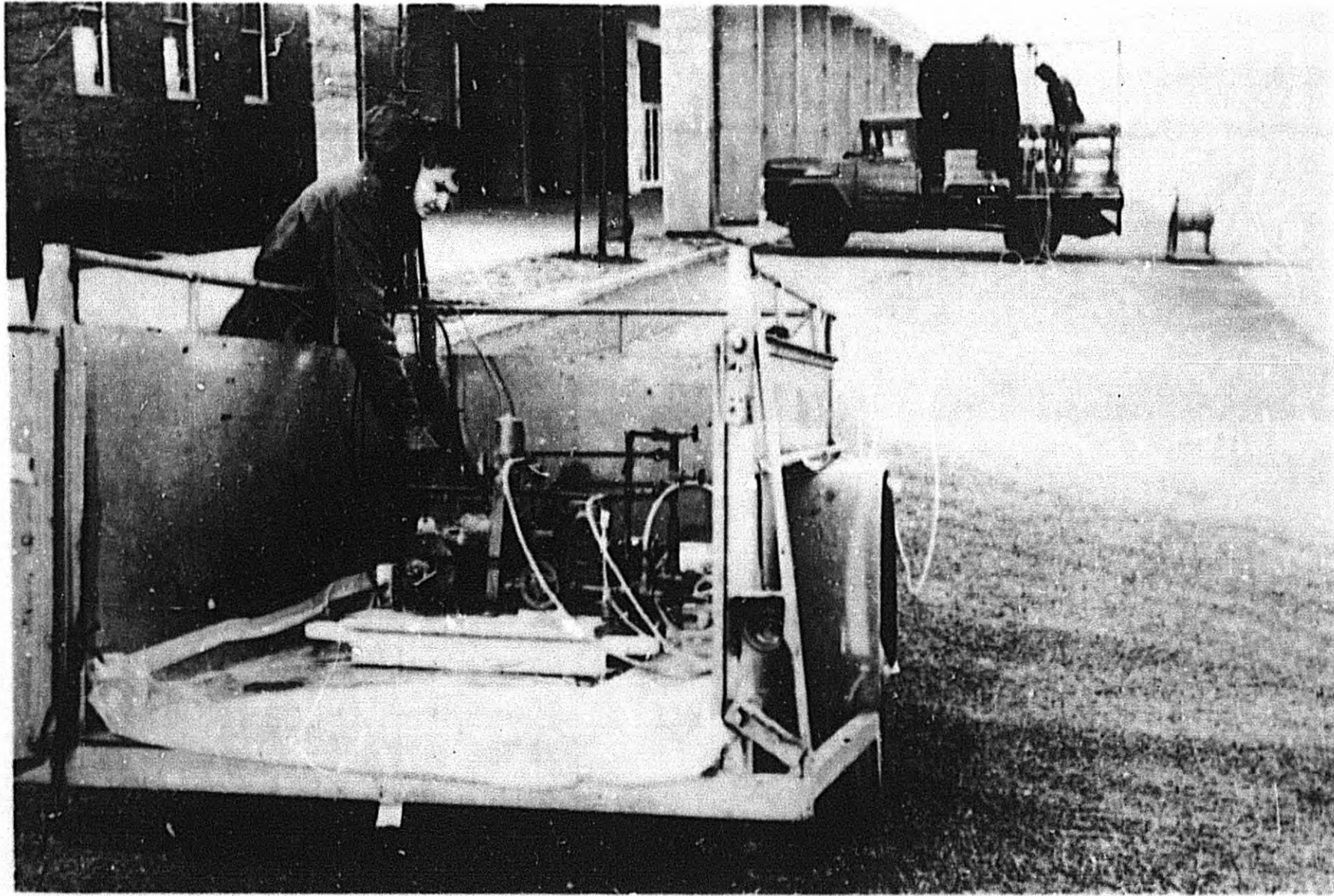


Fig. 2.4— Co^{60} source assembly.



20

Fig. 2.5—Remotely located source pumping system.

When the source has returned to the storage container, the piston enters a constriction, properly positioning the source so that a minimum radiation field exists at the surface of the container and further flow in the system is blocked. Then, either the pressure in the system will be allowed to rise gradually to 100 psi (well below the tubing burst pressure of 1000 psi), at which point the pressure-relief valve will trip and bypass the pump to the reservoir, or the solenoid valve will be returned to the free position, allowing return of the water to the reservoir. Under normal circumstances, while the source is being circulated, the internal pressure is approximately 20 psi.

The basic system is also equipped with several additional features designed to make the operation as foolproof as possible. These include (1) foreign-body filters on the pump intake tubes in the reservoir, (2) compression type fittings designed for high-pressure service, (3)

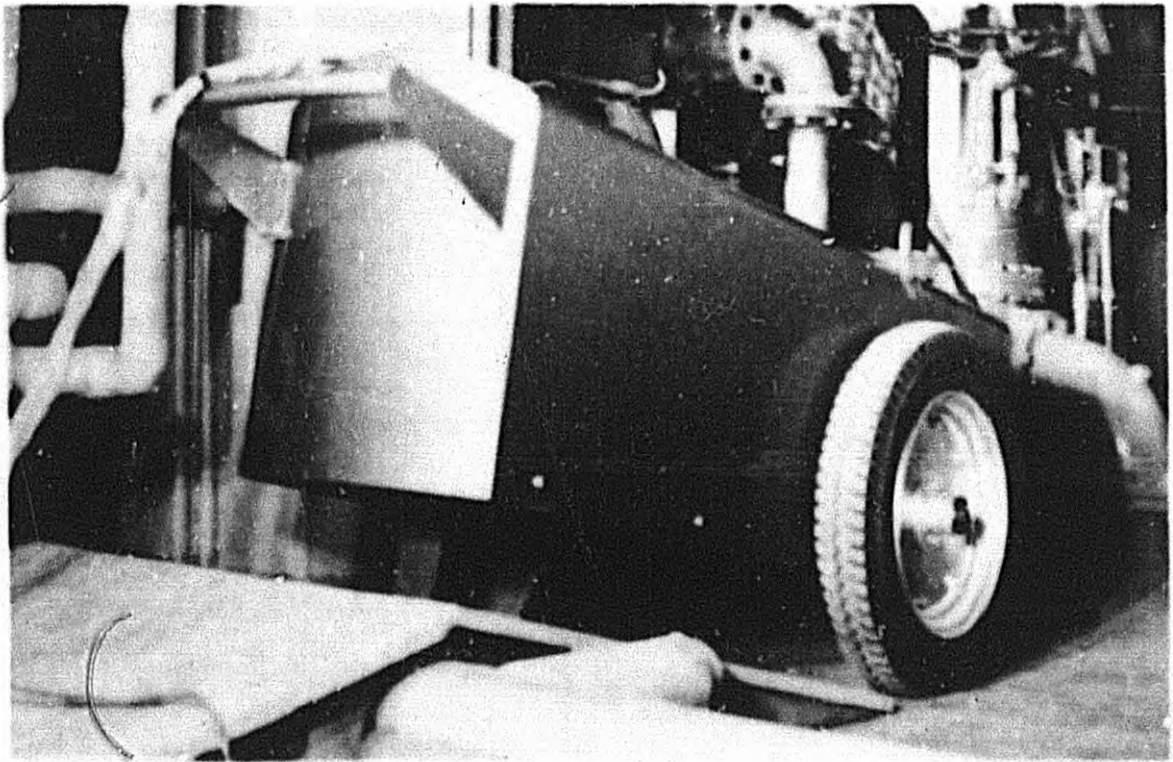


Fig. 2.6 — Radiographic unit used for point-source measurements.

antifreeze in the liquid to permit operation at subfreezing temperatures, (4) manually operated piston locks to hold the source assembly in place in its container while tubing is being connected or disconnected, (5) ball check valves to prevent reverse flow in the system, and (6) a piston trap designed to capture the piston at the end of its travel (its internal diameter is greater than that of the general system, permitting the piston leather to expand to a point where it is too large to reenter the tubing behind it).

2.1.2 Point-source Handling Equipment

An accurate evaluation of the protection afforded by the Headquarters building required the use of a relatively strong Co^{60} point source. The equipment selected to handle this multi-curie source was a TOI model 446 industrial radiographic unit, composed of a source container, a hand-powered source drive, and indicating devices (Fig. 2.6). The Co^{60} source, in metallic form, is encapsulated in a small container about the size of a cigarette filter. This is connected to a 50-ft-long flexible steel control cable that travels inside a plastic-covered flexible steel guide tube. The control cable passes over a crank-driven wheel in the control unit, which advances or retracts the source. This control unit contains an integral system of positive signal lights which indicates the source position at all times.

2.2 SOURCES

The gamma-energy spectrum of fallout¹⁻⁴ is not only complex but is also continuously changing with age. At about 1 hr after fission the radiation spectrum is such that the absorption in incremental slabs is similar to a monoenergetic beam of 1.25 Mev. During the following 24 hr the spectrum softens until, at about one day, it reaches an equivalent energy of about 0.7 Mev; thereafter harder components grow in until, at about 10 days, the spectrum once more behaves as though it were concentrated at 1.25 Mev. For purposes of the calculation of protection factors, it has become customary to assume this higher energy wherever simplification is necessary. The isotope Co⁶⁰ was therefore selected for the majority of the experiments reported here since its radiation spectrum consists of equal numbers of 1.17- and 1.33-Mev quanta. However, several experiments were also performed with an Ir¹⁹² source to obtain a measurement of the sensitivity of protection-factor determination to changes in gamma-ray energy.

The sources used in this experiment were (1) 198-curie Co⁶⁰, (2) 104-curie Ir¹⁹², and (3) 27-curie Co⁶⁰.

The first two sources were used for the simulation of plane radiation fields, and the third was used for point-source experiments. Metallic cobalt and iridium were prepared in the form of $\frac{1}{16}$ -in.-diameter by $\frac{1}{16}$ -in.-long cylinders, irradiated in the Materials Test Reactor, and then encapsulated at the TOI Arlington, Mass., Laboratory. Each source capsule (see Fig. 2.3) was attached to a stainless-steel wire rope approximately 13 in. long having at its far end a steel piston. The piston was fitted with a leather packing, similar to that of an old-fashioned pump, providing a seal to the inner surface of the tubing through which the assembly travels.

The third source was prepared in a similar manner. The source capsule (Fig. 2.7) was connected by a short length of flexible steel cable to a standard female cable connector used with existing industrial radiographic equipment.

2.3 SOURCE CALIBRATION

Calibration of the 27-curie Co⁶⁰ source was performed in a standard gamma-ray range established at the TOI Arlington laboratory. This range includes a highly stable scaled ionization chamber capable of reading dose rates up to 500 r/hr with a relative accuracy of ± 2 per cent and a set of marked positions at various distances from the chamber. Primary calibration of the range was accomplished by taking readings of a 100-millicurie Co⁶⁰ source, previously calibrated at the National Bureau of Standards (NBS), at each of the marked stations. As a check on accuracy, relative rates observed at these stations had been correlated with inverse-square attenuation and air scattering.

The larger sources of Co⁶⁰ and Ir¹⁹² were calibrated in a different manner. Because the quantity of fundamental interest was the relative response of the detector system to the sources, rather than the absolute strengths and sensitivities, a set of direct measurements was made to establish these relations. Then, after subsidiary measurements of detector sensitivity were made against the NBS calibrated source, nominal strengths were given to the two large sources.

Relative response was obtained in two ways for each source. In one experiment each source was set up at 50 and 100 ft from a vertical array of dosimeters (see Sec. 2.4); in a second experiment sources and dosimeters were attached to a long horizontal wire supported 8 ft above the ground, the distances between source and detectors varying from 50 to 150 ft. In all cases the sources were set at 8 ft above the ground. The horizontal traverse measurement permitted evaluation of the air and ground scatter reaching the detectors and therefore, by extrapolation, the establishment of a true relative strength that would actually be observed in vacuum. The data obtained from these experiments are presented in Fig. 2.8 for both the cobalt and the iridium sources. They are corrected for inverse-square attenuation, normalized to a standard date, and plotted against separation distance. Source strengths thus determined were 205 curies Co⁶⁰ and 306 curies Ir¹⁹², assuming 1.35 and 0.55 rhm/curie, respectively.

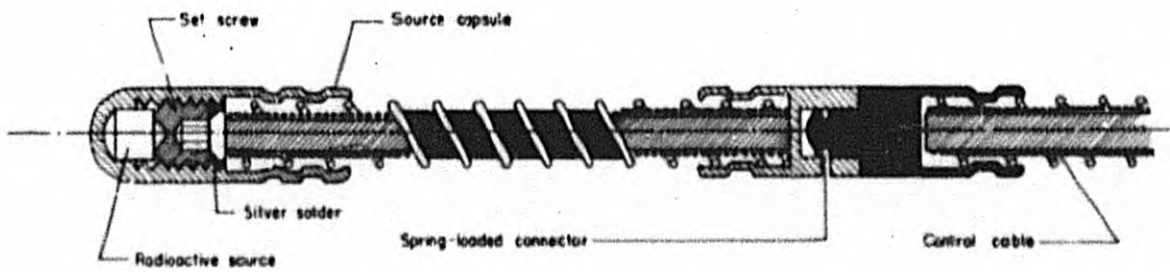


Fig. 2.7—Cutaway view of the 27-curie Co^{60} source capsule.

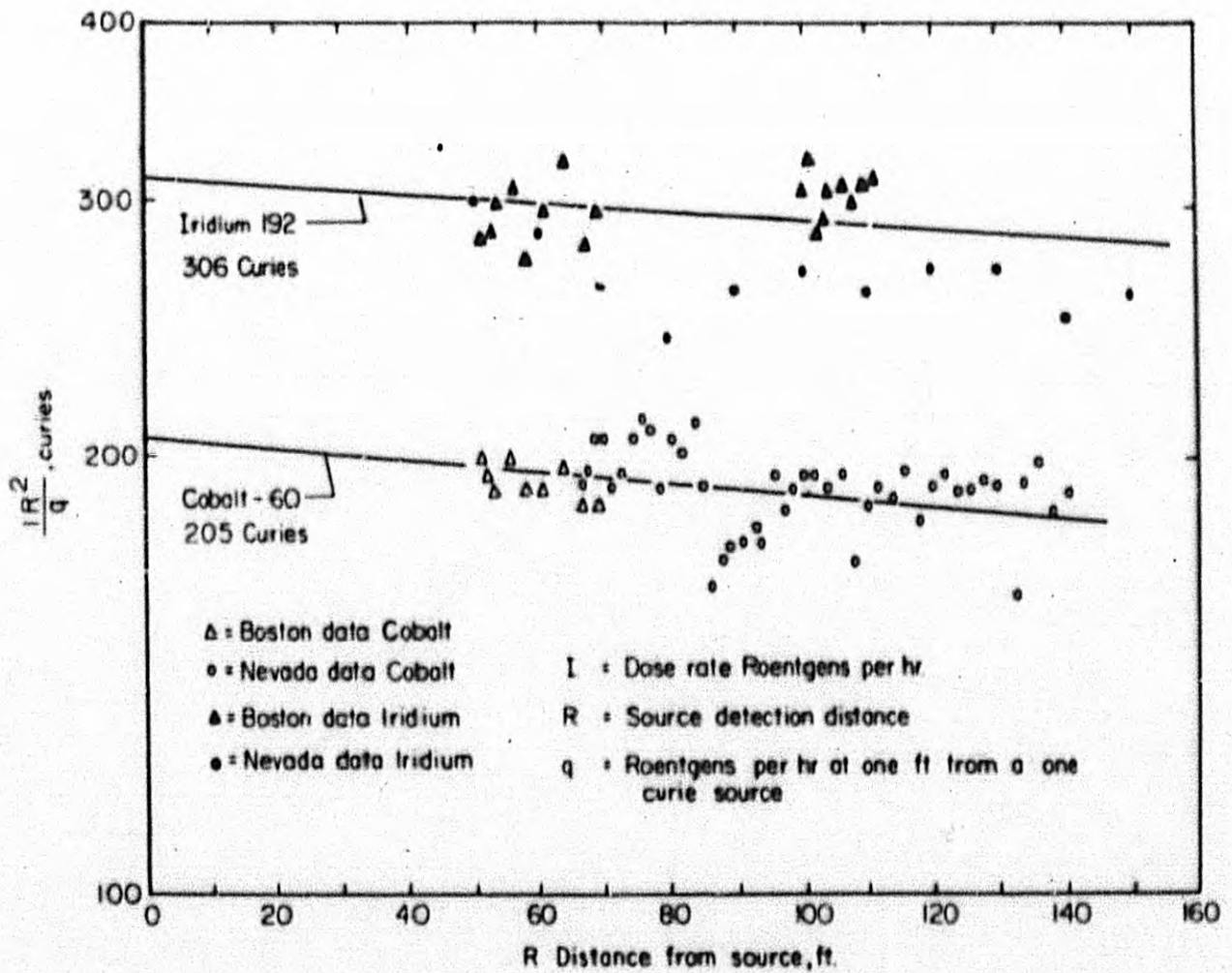


Fig. 2.8—Calibration curves for cobalt and iridium sources.

2.4 INSTRUMENTATION

Because the radiation field was simulated by moving a large single source over the prescribed area rather than by setting out a multitude of small sources, measurement had to be done with integrating detectors. For this reason, as well as their ready availability in large numbers and their isotropic and energy-independent response, pocket ionization chambers (PIC's) were selected for the purpose. Five hundred PIC's, Victoreen model 362, were obtained from the AEC Hanford Operations Office. When initially charged to 100 volts, the PIC's would record up to 250 mr dose before being completely discharged. Read-out was accomplished with five portable instruments specially constructed for the purpose⁵ (Fig. 2.9). Minimum detectable response with this dosimeter-reader system was about 1 mr.

The PIC's were calibrated by arranging them in circular fashion around a small Co^{60} source. In general, the dosimeters used in this experiment agreed within ± 2 per cent of each other and exhibited a leakage rate of less than 1 per cent per day. In order that this leakage rate might be kept as low as possible, frequent inspection of the drying capsules included in the base of each PIC was necessary. Since the sensitivity of an ionization chamber is directly proportional to the mass of gas contained within the chamber, corrections must be made for large changes in atmospheric pressure and temperature. However, the changes in pressure were found experimentally to be generally less than ± 0.2 in. Hg, and the temperatures indoors (where the PIC's were operated) remained constant to within $\pm 5^\circ\text{F}$. Consequently the correction factor turned out to be of the order of ± 1 per cent and was therefore neglected.

Since the experiments with a stationary source did not require radiation integration, the faster and more sensitive Victoreen model 592 ionization-chamber survey meters were used. These meters, capable of measuring dose rates at 10, 100, and 1000 mr/hr full scale, were calibrated with a known Co^{60} source before use. Their inverse feedback circuit provided a high degree of linearity and extremely short time response, permitting rapid, accurate measurements to be made.

Since the experiment control point of necessity (for reasons of personnel safety) was remotely located from the simulated radiation field, a remotely indicating radiation device was required to facilitate the timing of the experiment exposure. An on-off radiation measurement was all that was required for this purpose; therefore a TOI model 492 Gammalarm was selected. This instrument provides a visual indication (a steady green light if the field is below 2 mr/hr and a flashing red light if higher) and has a power outlet that is energized if the field is above 2 mr/hr. The instrument was located in the simulated radiation area at a point where the field would always be above 2 mr/hr when the source was exposed. An extension cord from the power outlet of the instrument was connected to an experiment timer and visual indicating device in the control-point area. Figure 2.10 illustrates the operation of this device. The Gammalarm was also useful as an indicator to warn of the presence of radiation during experiments; its red flashing light could be seen for some distance, particularly at night when most of the work took place.

2.5 EXPERIMENTAL TECHNIQUE

The experimental technique devised consisted in measuring the radiation field produced by a simulated contaminated area of known source strength surrounding the structure. This contaminated field is simulated by moving a single source at constant speed over the area of interest (Figs. 2.11 and 2.12) in such a manner that the source spends the same time interval per unit area throughout the area to be simulated. Thus, by the use of time-integrating detectors at selected points within the structure, the effective radiation was made to appear as arising from an area source. This technique has the advantage of averaging out local effects of the terrain and the structure under test in much the same way as would a true fallout field.

Whenever possible, the symmetry of the structure under investigation was used to reduce the area over which it was necessary to lay out the source tubing. Thus, for a survey of structures with a line of symmetry down the center, such as the wing of a building, the simulated fallout pattern was laid out on the ground on only one side, and detectors were placed sym-

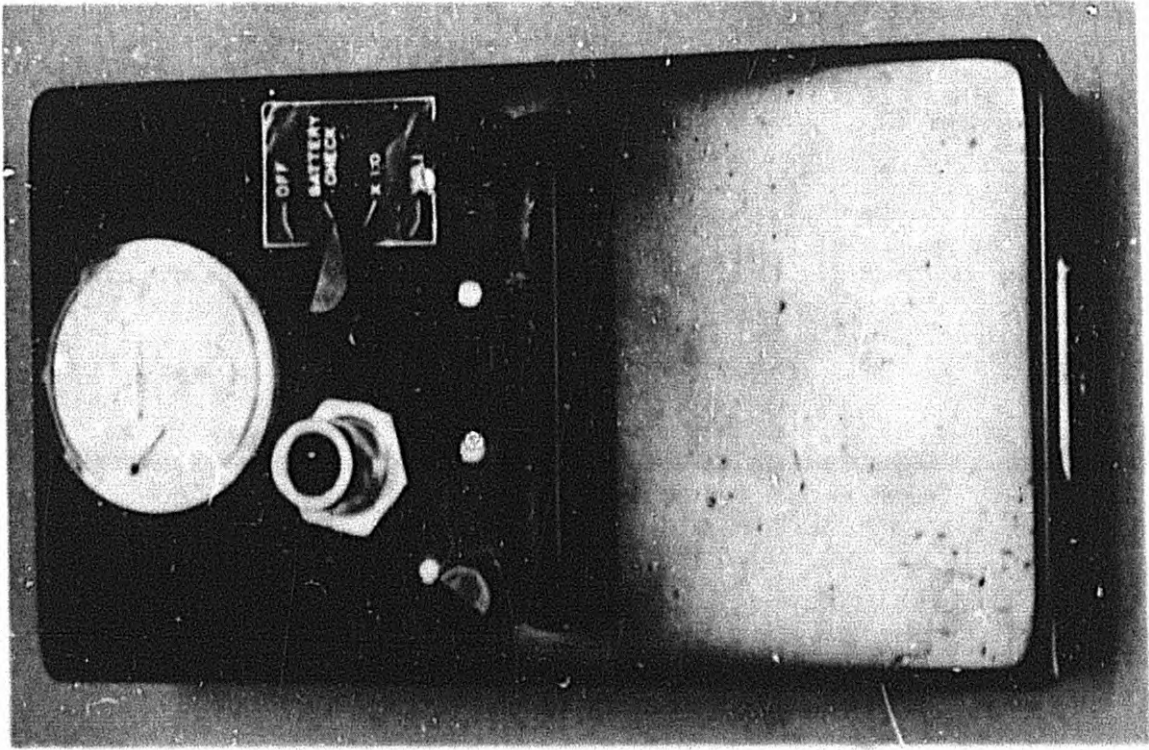


Fig. 2.9—PIC reading instrument.

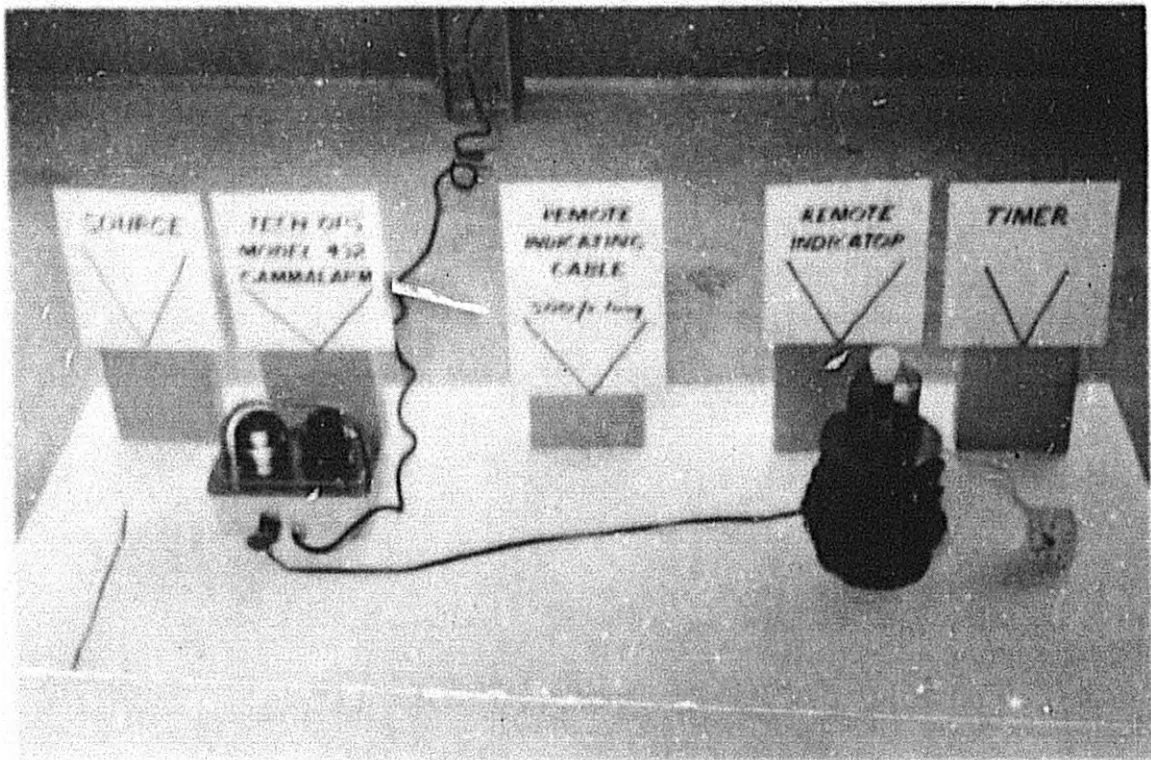


Fig. 2.10—Mock-up of remote radiation indicating device.

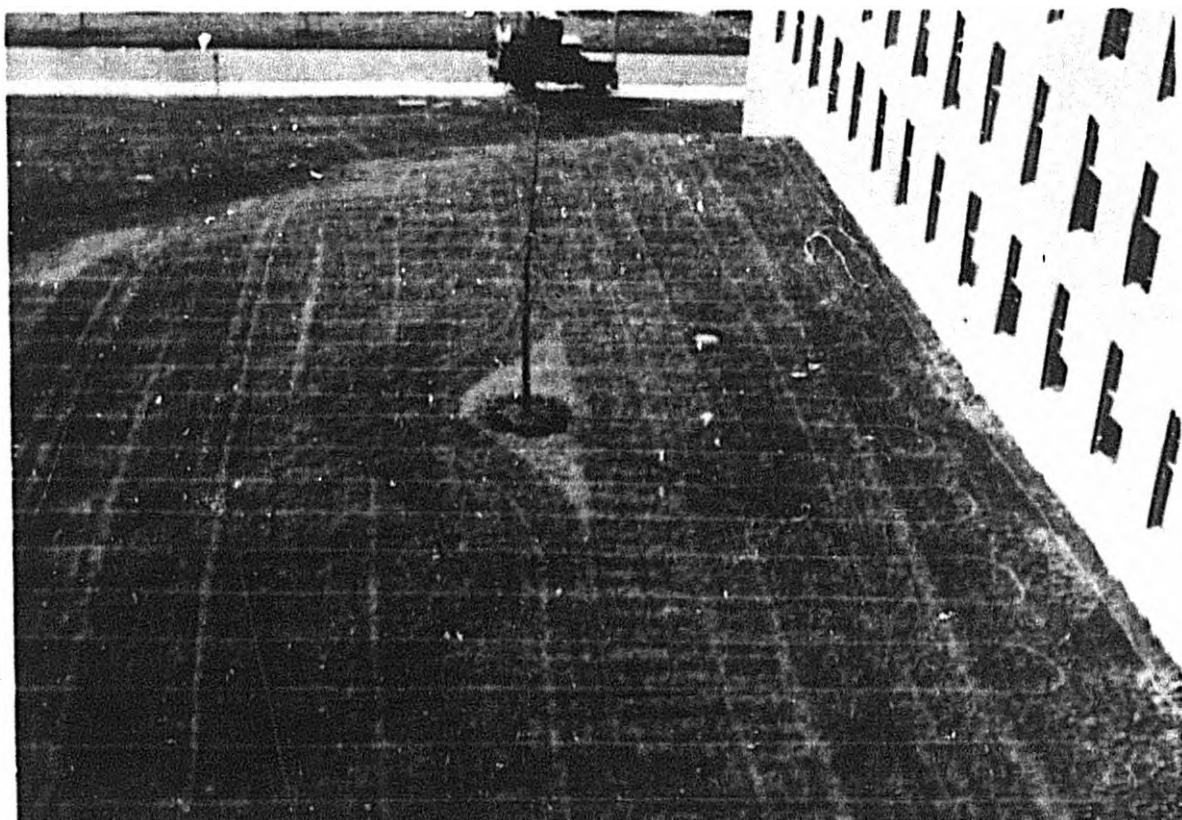


Fig. 2.11—Simulation of a uniform rectangular radiation field.

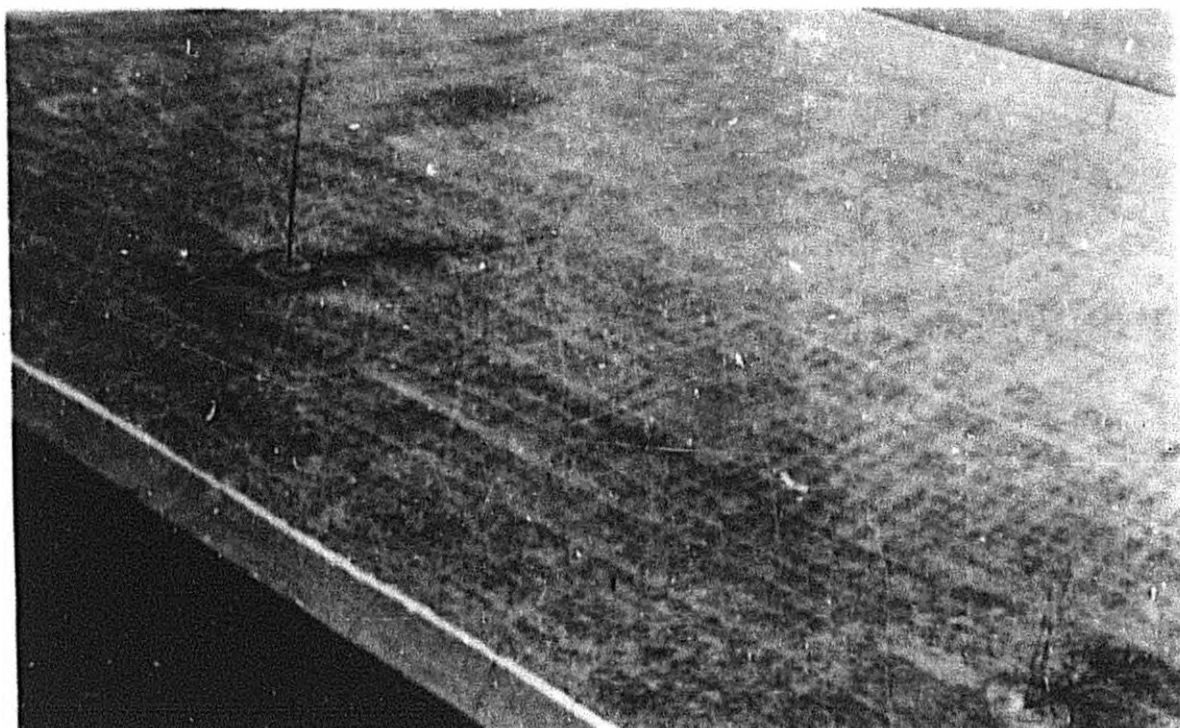


Fig. 2.12—Simulation of a semicircular field of constant source density.

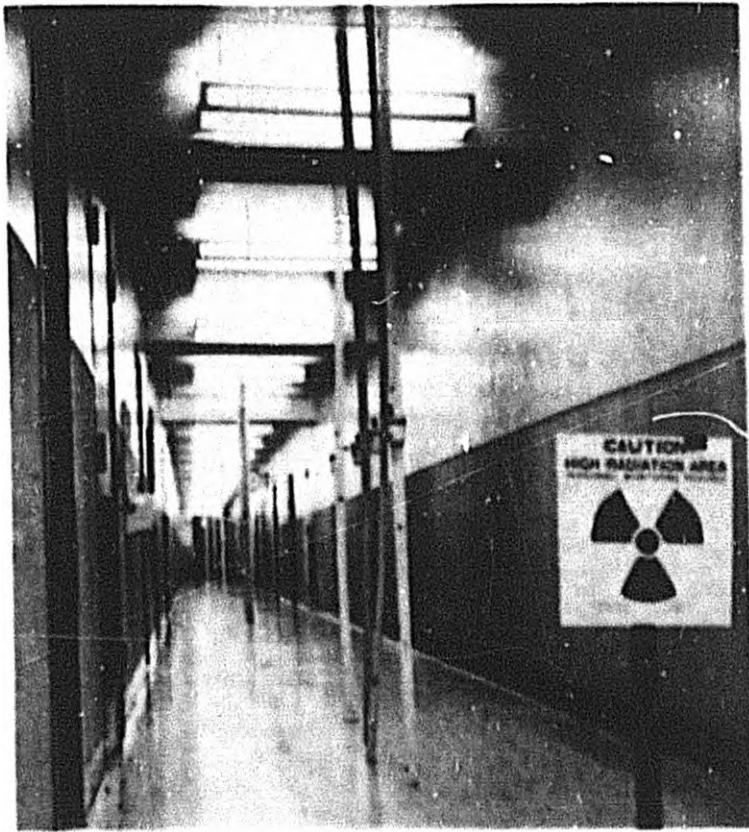


Fig. 2.13—Hall instrumentation, illustrating placement of PIC's.

R

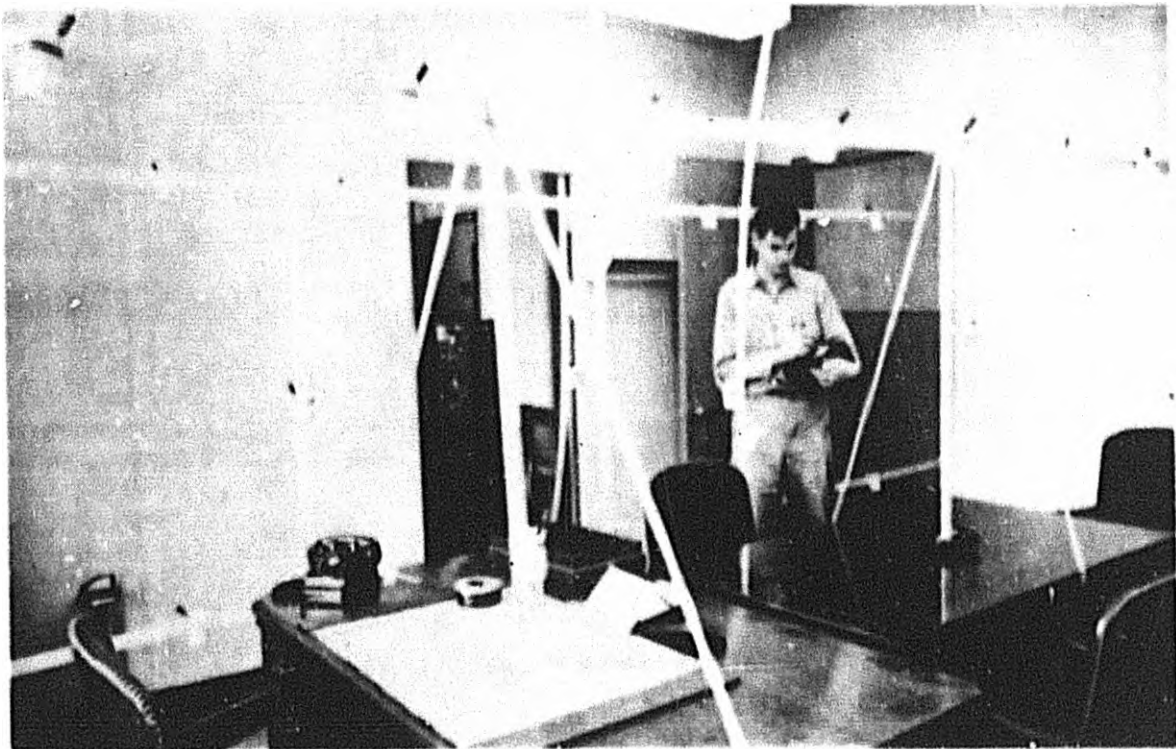
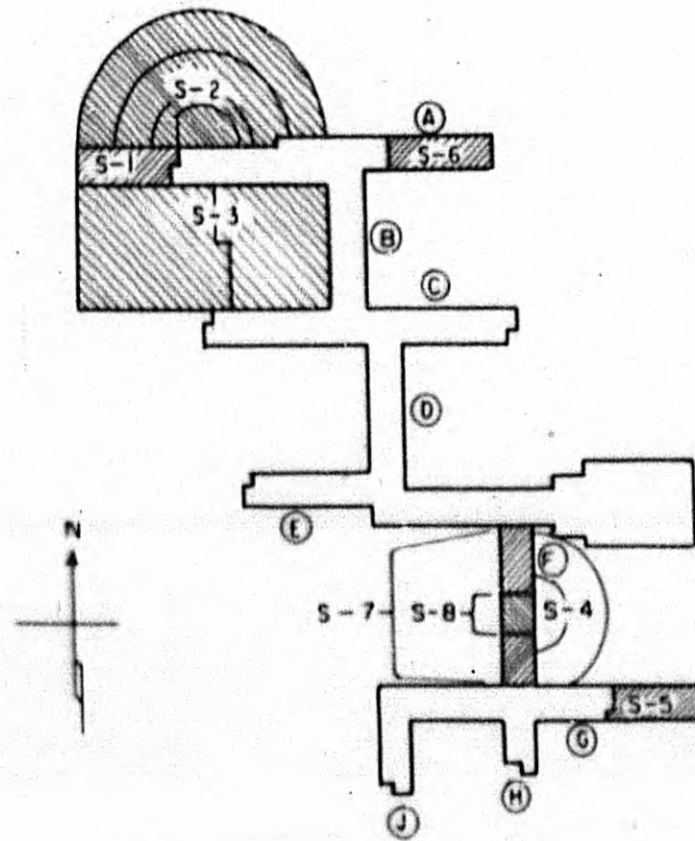


Fig. 2.14—Office instrumentation, illustrating placement of PIC's.



SUN	MON	TUE	WED	THUR	FRI	SAT
	1		FEB 11	12	13	14
	3			1		3
						1
3			3		2	2
		3		3		
				Point source exps.		
22	23	24	25	26	27	28
4		5			5	6 7
2		Point source exps.	4		Point source exps.	5
MAR 1	2	3	4	5	6	7
2		8			6	
2	7		8		Point source exps.	6

Fig. 2.15—Experiment schedule and locations.

metrically across the building so that readings would be added. In this way the same results were obtained as would have been achieved from a complete field.

A typical test with the simulated area source consisted in the following steps. First, a rough calculation or estimation of the source density required to yield significant accumulated dosages was made. Second, based on this estimation the polyethylene tubing through which the source travels was distributed to produce the required field, and a dummy source (containing no activity) was circulated to ensure that the tubing had not been damaged. Third, about 1 hr before the test was started, dosimeters were charged and placed in their preplanned locations. Dosimeters were placed in paper cups attached to wooden laths sprung between floor and ceiling (Figs. 2.13 and 2.14). This system allowed obstructing dosimeter arrangements to be removed before working hours.

When radiological-safety clearance was given, the tubing was connected to the storage containers, and the system was energized. The test times ranged from a minimum of 1 hr to about 10 hr, depending upon the exposure desired. At the conclusion of a test exposure, the source was returned to its container and properly secured. Thereafter the dosimeters were read and recorded, and the source tubing was picked up for use in the next experiment. Figure 2.15 indicates the experiment schedule that was established.

Experiments were also performed with a 27-curie cobalt point source to determine the effect of localized fallout concentrations in the basement shelter area. The locations where it was believed fallout would concentrate were either air filters or roof drains. The test procedure used was to survey the area surrounding a point of interest and mark off a 10-ft-square grid. Next, the source container was placed in position so that the source could be projected to the desired location. After the test area was roped off at all entrances where the field was expected to exceed 2 mr/hr, the source was exposed, and readings of dose rate were made at the cross points of the 10-ft grid with a Victoreen model 592 survey meter. At the completion of the test the source was secured in its storage container, and all barricades were removed.

REFERENCES

1. L. V. Spencer and J. H. Hubbell, Report on Current Knowledge of Shielding from Nuclear Explosions, Report NBS-5659, November 1957.
2. R. C. Bolles and N. E. Ballou, Calculated Activities and Abundances of U^{235} Fission Products, Report USNRDL-456, August 1956.
3. C. F. Miller, Gamma Decay of Fission Products from the Slow-neutron Fission of U^{235} , Report USNRDL-TR-187, July 1957.
4. A. T. Nelms and J. W. Cooper, U^{235} Fission Product Decay Spectra at Various Times After Fission, Health Physics, 1: 427 (1959); and Report NBS-5853, April 1958.
5. E. T. Clarke et al., Measurement of Attenuation in Existing Structures of Radiation from Simulated Fallout, Report TOB 59.4, Apr. 2, 1959.

Chapter 3

PRESENTATION OF DATA

3.1 AREA-SOURCE EXPERIMENTS

Fixed radiation fields were simulated at eight different locations around and within the building. Figure 3.1 shows the location of each of these with respect to a plan view of the building. The parameters pertinent to each experiment are summarized in Table 3.1. The data obtained from the experiments utilizing Co^{60} were normalized¹ to milliroentgens per hour from a mean source strength of 0.062 megacurie per square mile, a density which, if infinite in extent, would produce a field of 1000 mr/hr at 1 meter above it. The data obtained from the experiments utilizing Ir^{192} were normalized to milliroentgens per hour from a mean source strength of 0.151 megacurie per square mile.

All the normalized experimental data are presented in Figs. 3.2 to 3.7 in tabular form together with a floor plan of the area of the building being tested. The locations of the dosimeters and room partitions for each floor are noted on these floor plans. Unless otherwise specified, all data represent measurements at 4 ft above the floor.
















3.2 POINT-SOURCE DATA

In the basement shelter area, there are several fallout traps in unshielded locations which would emit radiation in the event of an actual attack. These were, in general, either emergency air filters or exposed roof drains. The effect of these fallout traps in the shelter area was examined by placing a 27-curie Co^{60} source where fallout was expected to accumulate and measuring the resultant radiation field with a Victoreen model 592 survey meter. The data obtained from these experiments are given on basement floor plans as dose-rate contours in milliroentgens per hour per curie together with the appropriate source locations (Figs. 3.8 to 3.16). The basement values are represented by the solid-line contours, and the first floor, by the broken-line contours.

Since the locations of the air filters and roof drains were such that, for significant fallout collection, a large percentage of the shelter area would be rendered useless, experiments were performed to indicate feasible, safe alternate positions. In general, it was determined that a considerable improvement in shelter capability could be achieved by relocating the air filters in their respective plenum chambers outside the main basement walls. Figures 3.10, 3.15, and 3.16 give the radiation contours that would be obtained from this relocation.

In addition, one experiment was performed with the large 100-curie cobalt source to investigate further the effect of far-field radiation. The results of this experiment, in which the source was placed 200 ft east of the center line of wing F, are given in Fig. 3.6 together with the area-source measurements for the same location.

TABLE 2.1—AREA-SOURCE EXPERIMENTS

Experiment No.	Location*	Source	Curie
F-1	West side of wing A, 0 to 200 ft		100
F-2	North side of wing A, 0 to 112 ft		100
F-3	North side of wing A, 112 to 198 ft		100
F-4	North side of wing A, 198 to 200 ft		100
F-5	North side of wing A, 0 to 80 ft		100
F-6	West side of wing B, to change in ground level		100
F-7	West side of wing B, from change in ground level to 420 ft		100
F-8	East side of wing F, 0 to 80 ft		100
F-9	East side of wing F, 80 to 112 ft		100
F-10	Point source, 200 ft east of center line of wing F		100
F-11	East side of wing G, 0 to 200 ft		100
F-12	Roof on east side of wing A		100
F-13	Roof of wing F		100
F-14	Roof of wing F		104
F-15	First floor, 60- by 40-ft area centered about center line of wing F		100

* See Fig. 2.1.

REFERENCE

1. J. A. Auxier et al., Experimental Evaluation of the Radiation Protection Afforded by Residential Structures Against Distributed Sources, Report CEX-58.1, Jan. 10, 1959.

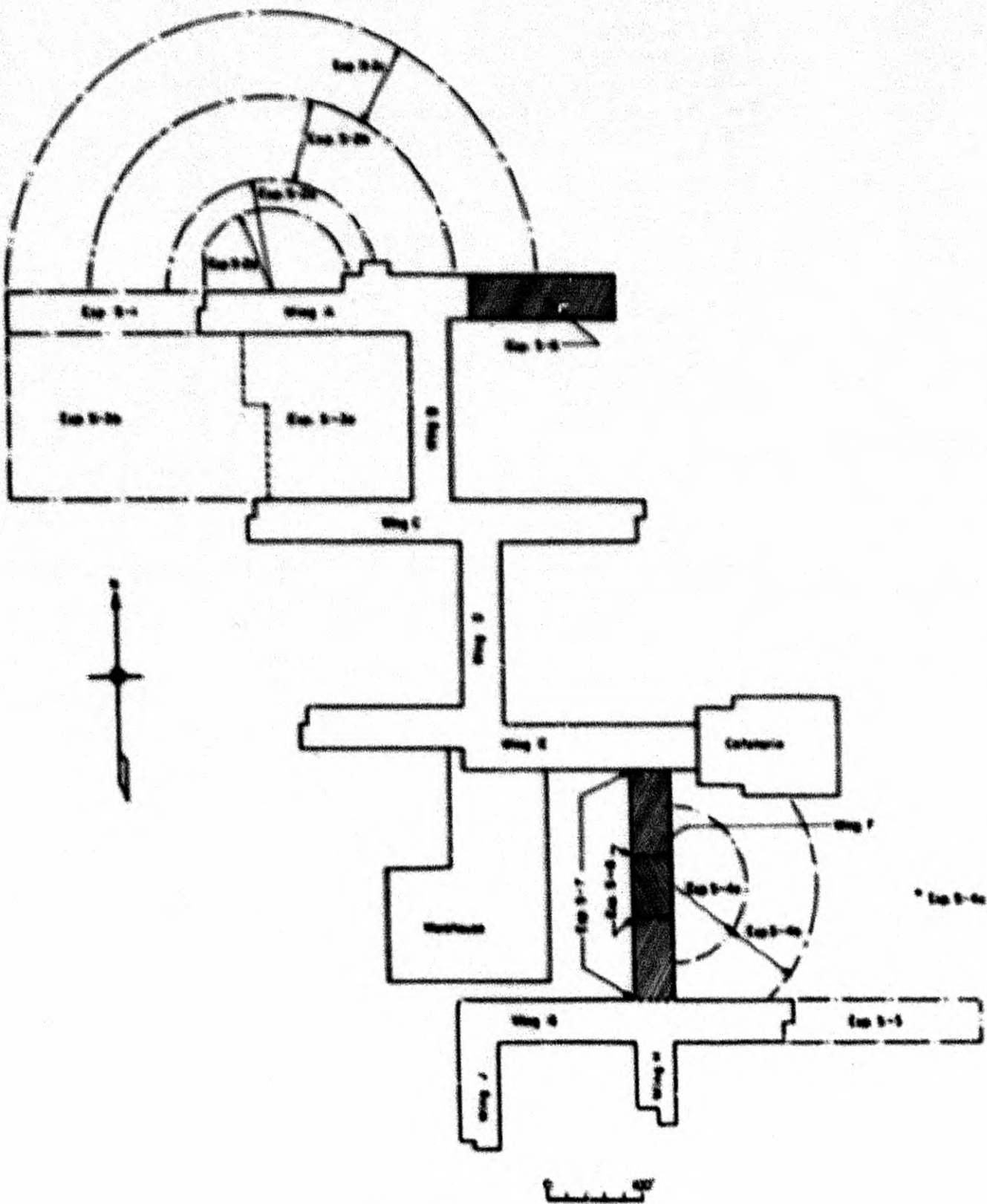
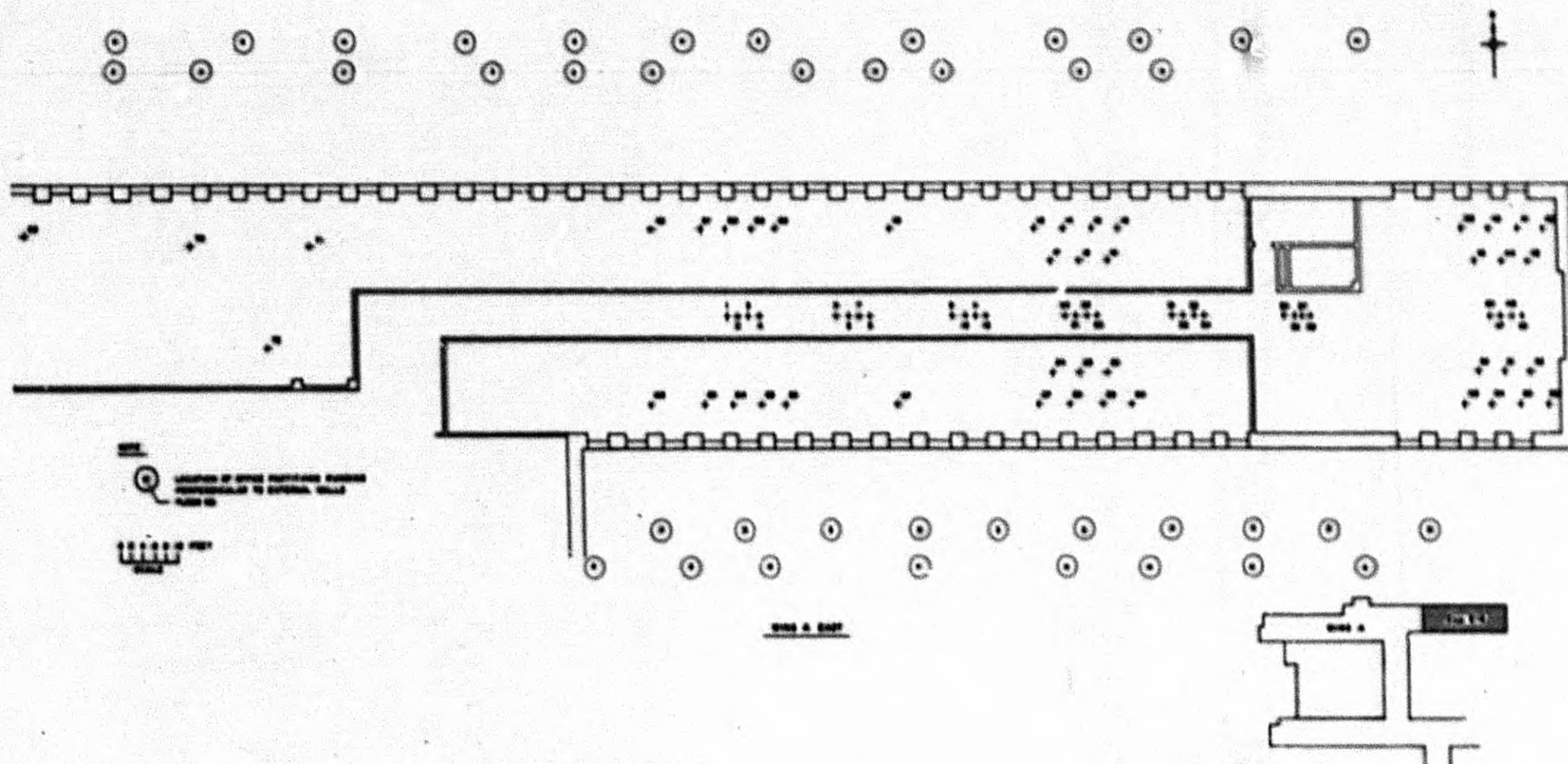


Fig. 3.1—Location of area experiments.

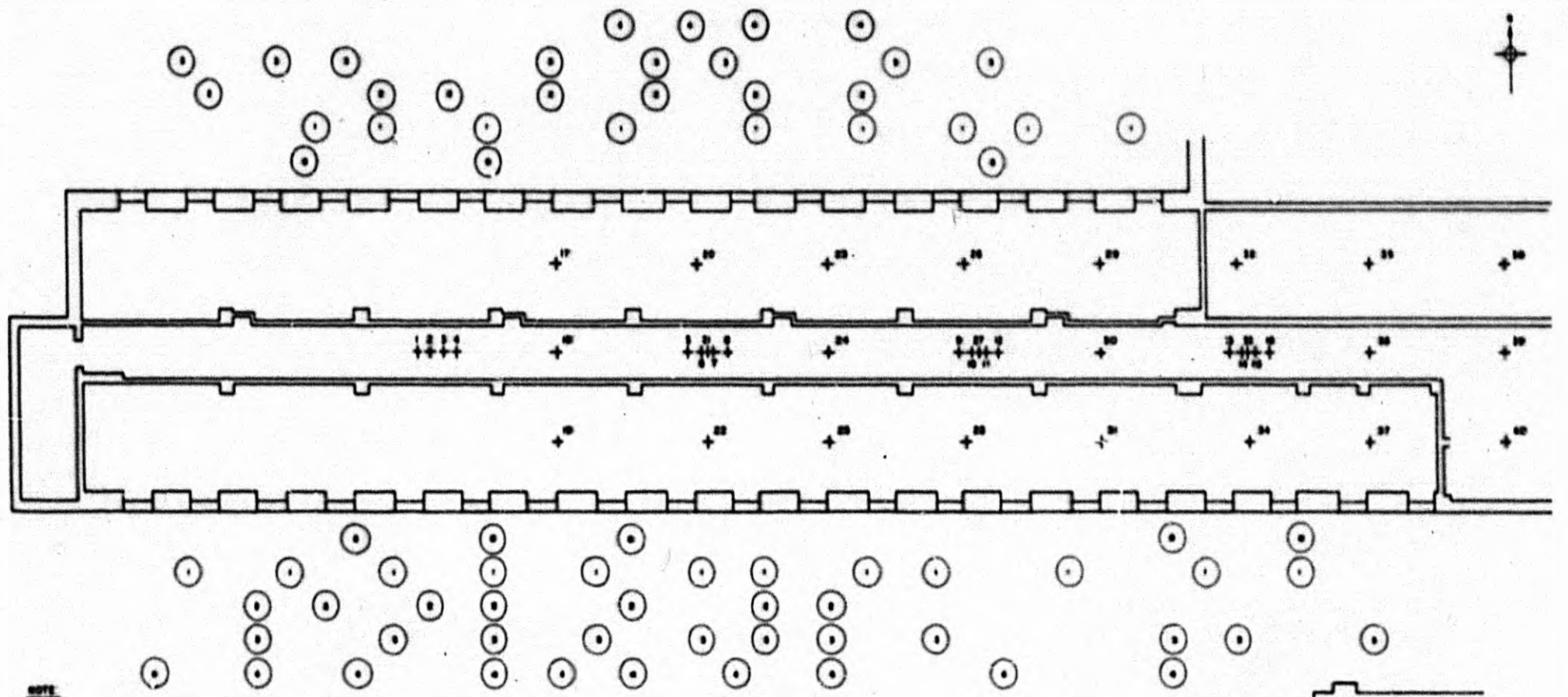


Experiment 8-6 Position	1	2	3	4	5	6	7	8	9	10	11	12	13	14	15	16	17	18	19	20	21	22	23	24	25	26	27	28	29	30	31	32	33	34	35	36
Third Floor	.084	.076	0	0	.16	.29	.16	.28	.28	.33	.27	.33	.19	.30	.28	.21	.32	.22	.27	.25	.19	.16	.20	.32	.28	.25	.29	.33	.22	.16	.28	.16	.25	.17	.14	
Fourth Floor	4.7	4.7	6.1	7.4	12	12	12	12	12	13	13	13	13	13	13	13	13	13	13	13	13	13	13	13	13	13	13	13	13	12	12	12	12	12	11	11

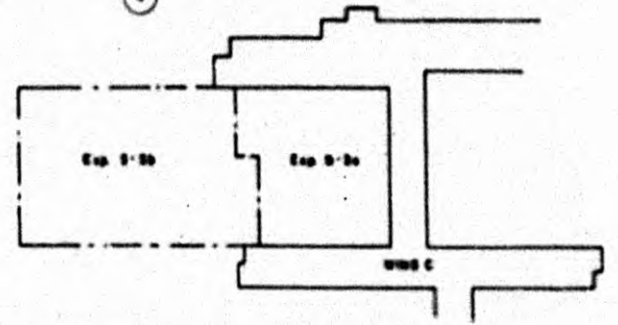
Experiment 8-6 Position	37	38	39	40	41	42	43	44	45	46	47	48	49	50	51	52	53	54	55	56	57	58	59	60	61	62	63	64	65	66	67	68	69	70	71	72	
Third Floor	.093	.075	.23	.18	.18	.15	.19	.26	.16	.24	.19	.19	.20	.27	.27	.24	.30	.33	.24	.037																	
Fourth Floor	11	11	9	9	9	9	10	10	10	9	9	9	9	9	12	12	12	10	10	10	10	7	9	12	12	4	3	4	9	7	9	12	3	0	0	0	

Fig. 3.3—Normalized data for wing A east.

88



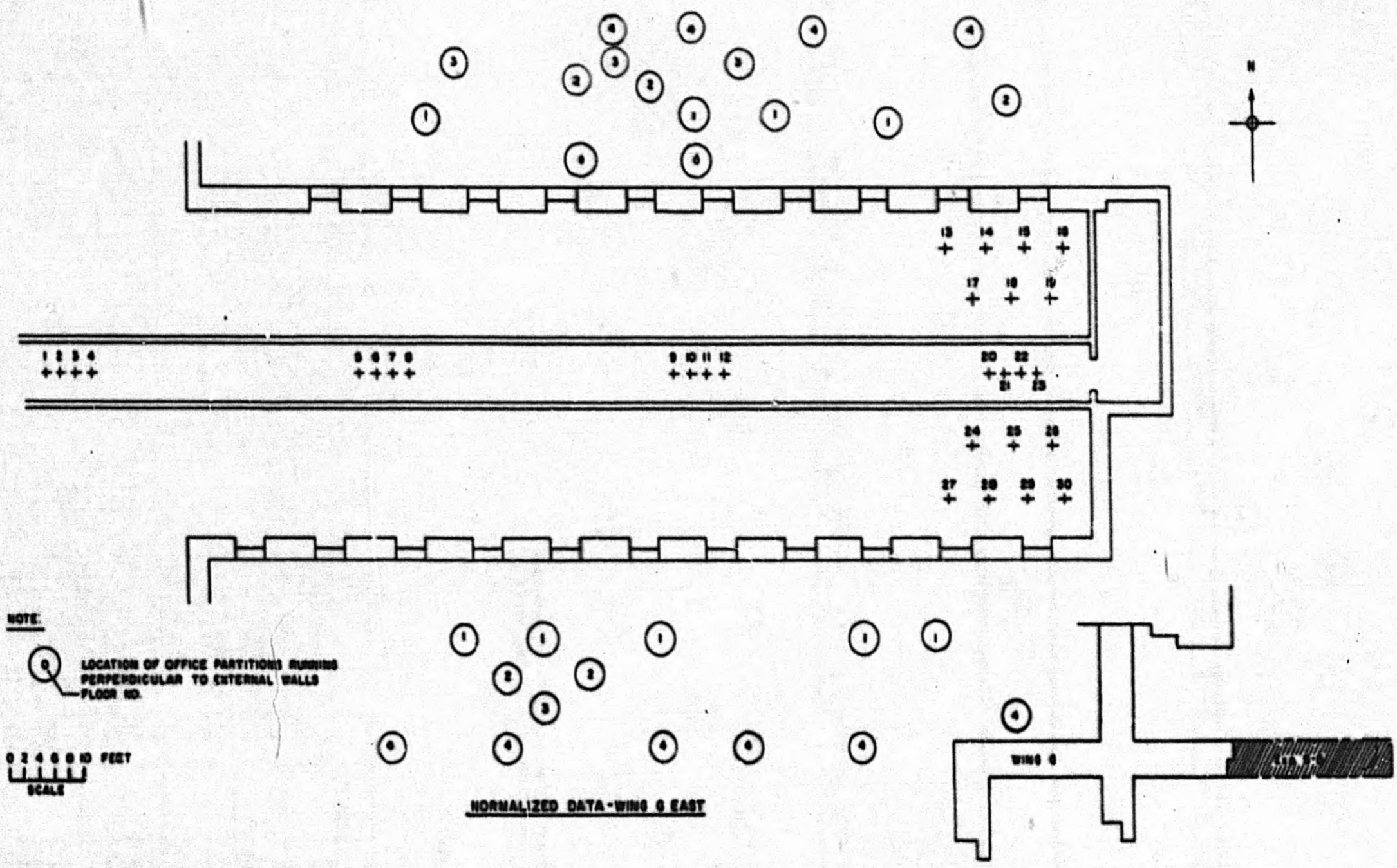
NOTE
 (○) LOCATION OF OFFICE PARTITIONS CIRCLES
 PERPENDICULAR TO EXTERNAL WALLS
 FLOOR IS



WING C

Experiment	Position	1	2	3	4	5	6	7	8	9	10	11	12	13	14	15	16	17	18	19	20	21	22	23	24	25	26	27	28	29	30	31	32	33	34	35	36	37	38	39	40		
Ground Floor	3-2a																	.90	.81	.82	.65	.84	.89	.80	.020		.85	.020	0	.85	.12	.12		.21	.20	.20	.20	.20	.21	.40	.41		
First Floor	3-2a	10	10	4.2	3.3	4.2	5.0	5.4	5.0	6.2	4.2	4.2	4.2	4.2	0	0	0																										
	3-2b	.22	.65	.22	.22	.15	0	.68	0	.18	.10	0	0	.16	0	0																											
Second Floor	3-2a	0	.42	.04	.62	.04	.04	1.3	.42	.04	.42	.42	.04	0	0	0																											
	3-2b	.16	.19	.19	.19	.16	.26	.25	.16	0	0	0	.032	0	0	0																											
Third Floor	3-2a	.04	.04	0	0	.42	.04	.04	.42	1.3	.42	1.7	1.7	0	.42	0	0																										
	3-2b	0	.23	0	0	0	0	0	.16	.040	0	.16	.26	0	.13	0	0																										
Fourth Floor	3-2a	.04	.04	.04	.04	0	.04	.42	0	0	0	0	0	0	0	0																											
	3-2b	.22	.26	.25	.26	.19	.18	.097	.11	.040	.12	.26	0	.20	.097	.42	.12																										

Fig. 3.5—Normalized data for wing C west.



Experiment	Position	1	2	3	4	5	6	7	8	9	10	11	12	13	14	15	16	17	18	19	20	21	22	23	24	25	26	27	28	29	30
S-5	Basement	0	0	0	0	0	0	0	0	0	0	0	0	0	0	.032	.018	0	0	0	0	.080	0	0	0	.044	.044	0	0	.044	.032
S-5	First Floor	-	.010	0	0.05	0	0	0.14	0	0	0	.12	.01	.020	.14	.13	.11	.040	.050	.24	.17	.28	.31	.38	.21	.28	.36	0.22	.37	.60	.86
S-5	Second Floor	0	0	0	0	0	0	0	0	0	0	0	0	.028	.016	.040	.018	0	.010	.040	.012	.068	.040	.098	-	-	-	-	-	-	-
S-5	Third Floor	0	0	0	0	0	0	.012	0	0	0	0	0	.016	0	.032	0	0	.024	0	.020	.044	.052	-	-	-	-	-	-	-	-
S-5	Fourth Floor	0	0	0	0	0	0	0	0	0	0	0	0	.032	0	0	0	0	0	0	0	0	.056	.032	.032	.056	.098	.040	.040	.066	.12

Fig. 3.7—Normalized data for wing G east.

39

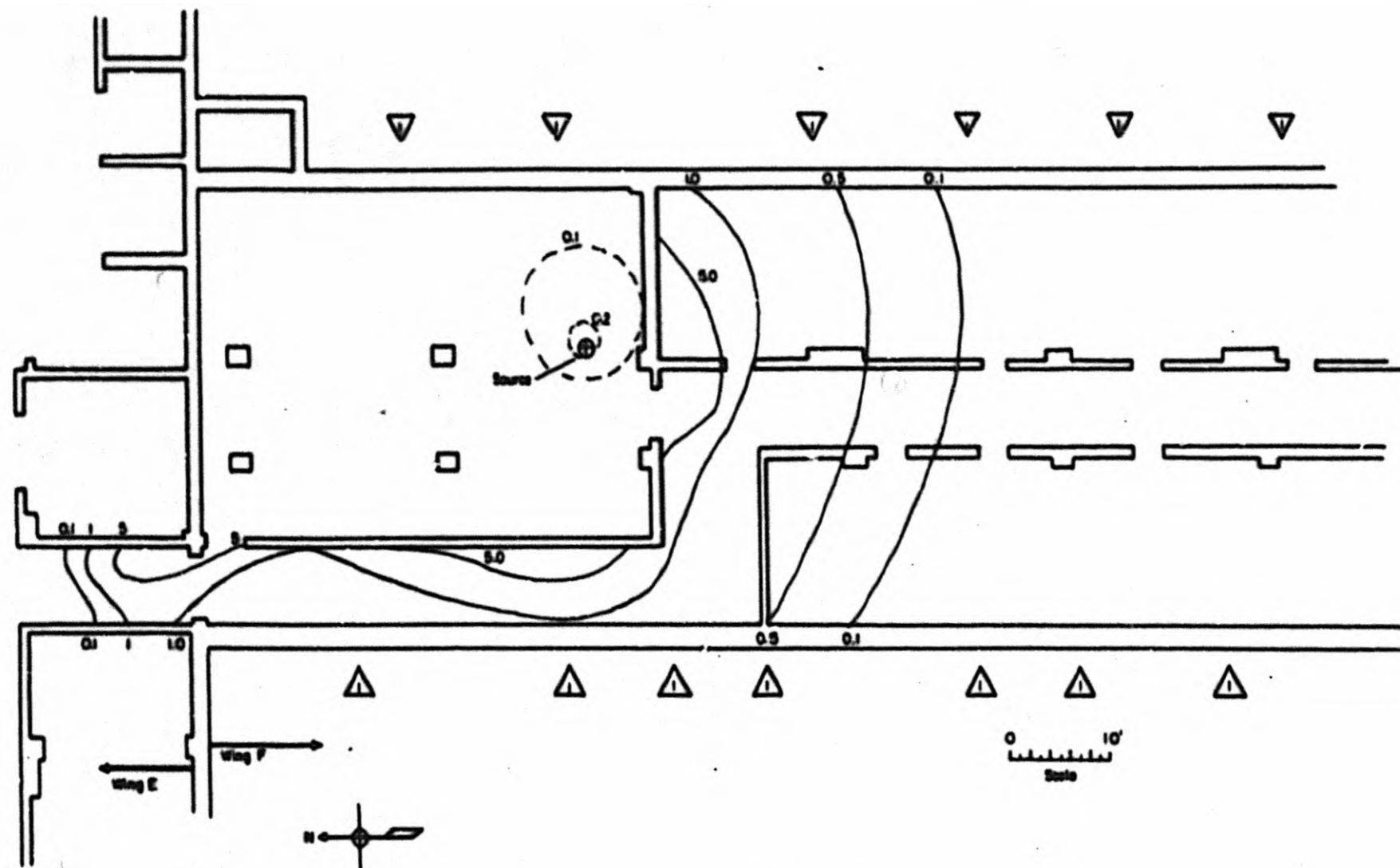


Fig. 3.8—Point source below air filter in wing F. —, Basement values, mr/hr/curie. - - -, First-floor values, mr/hr/curie. ▽, Locations of office partitions running perpendicular to external walls on the first floor.

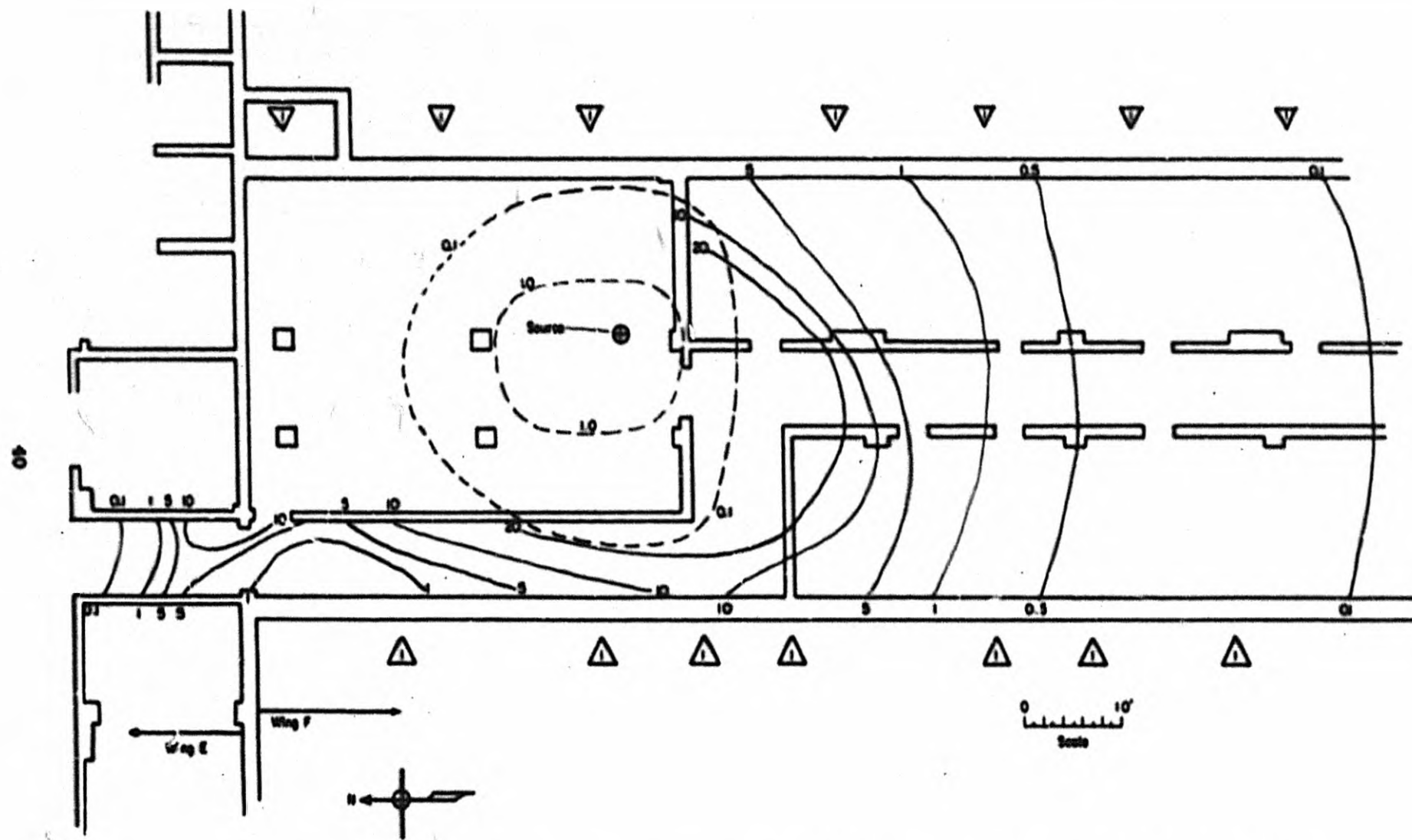


Fig. 3.9—Point source above air filter in wing F. —, Basement values, $\text{m}^2/\text{hr}/\text{curie}$. - - -, First-floor values, $\text{m}^2/\text{hr}/\text{curie}$. ∇ , Locations of office partitions running perpendicular to external walls on the first floor.

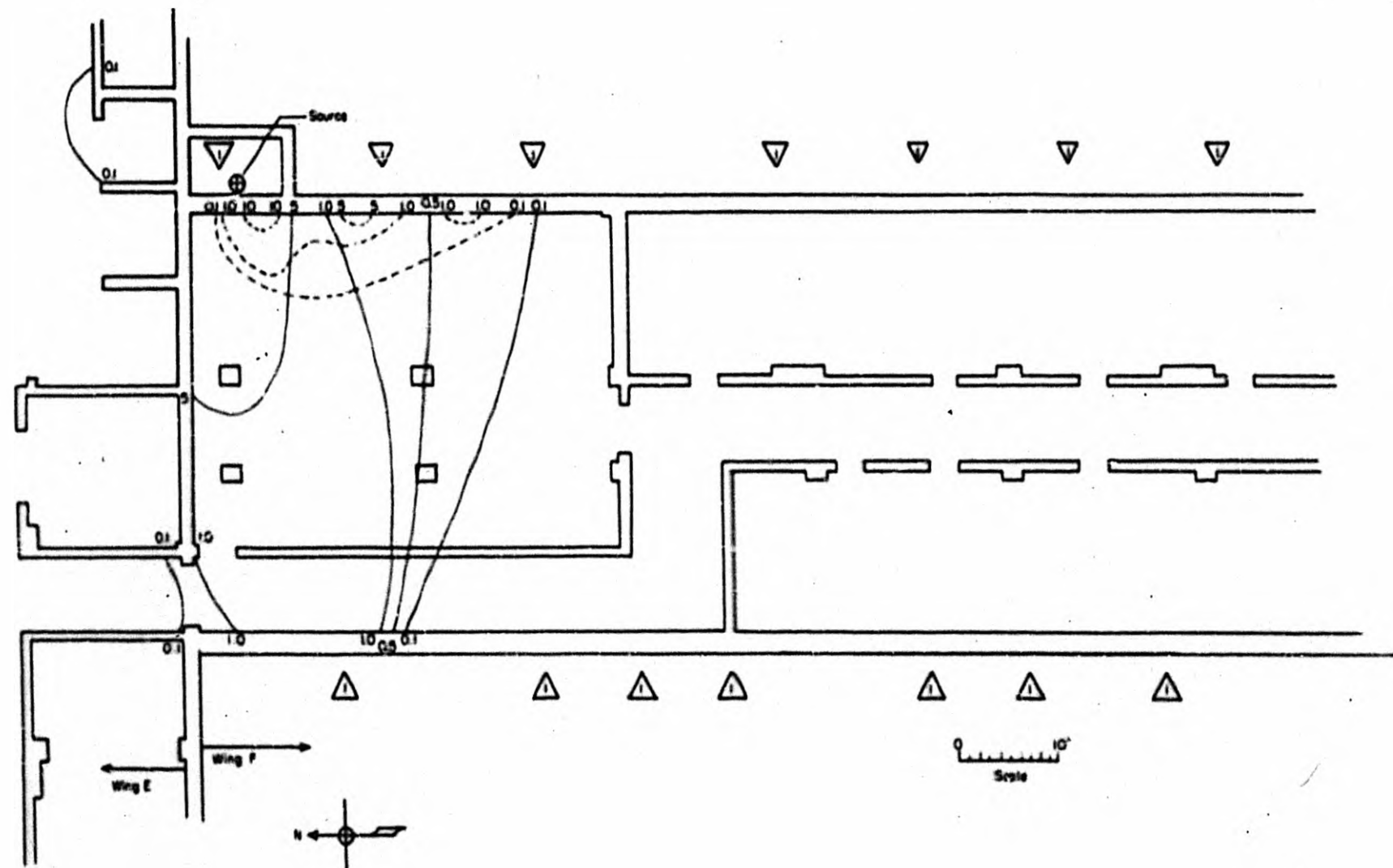


Fig. 3.10—Point source located at emergency air inlet in wing F. —, Basement values, mR/hr/curie. - - -, First-floor values, mR/hr/curie. ▽, Locations of office partitions running perpendicular to external walls on the first floor.

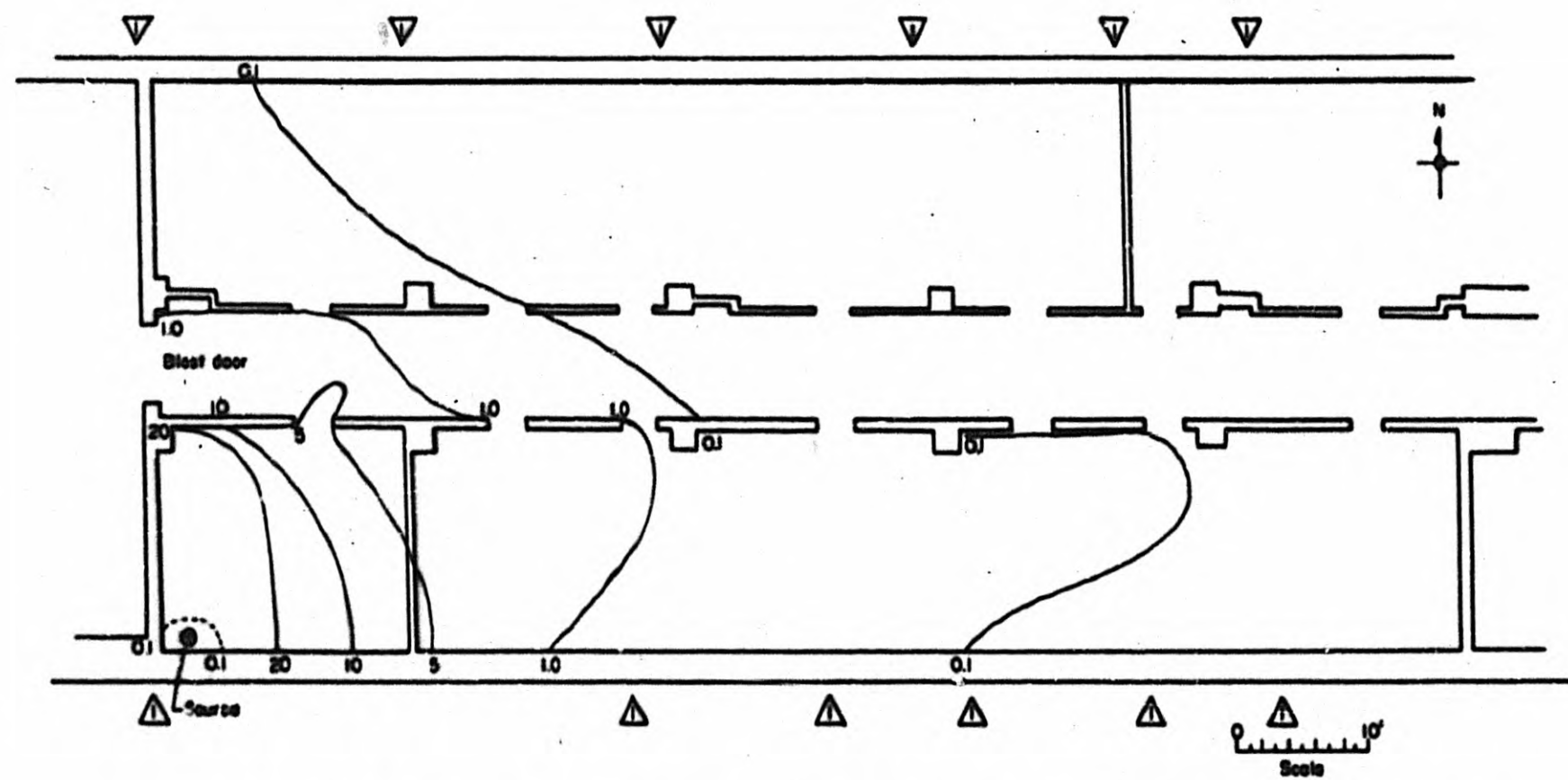


Fig. 3.11—Point source below roof drain in wing C. —, Basement values, $\text{m}^2/\text{hr}/\text{curie}$. - - -, First-floor values, $\text{m}^2/\text{hr}/\text{curie}$. ∇ , Locations of office partitions running perpendicular to external walls on the first floor.

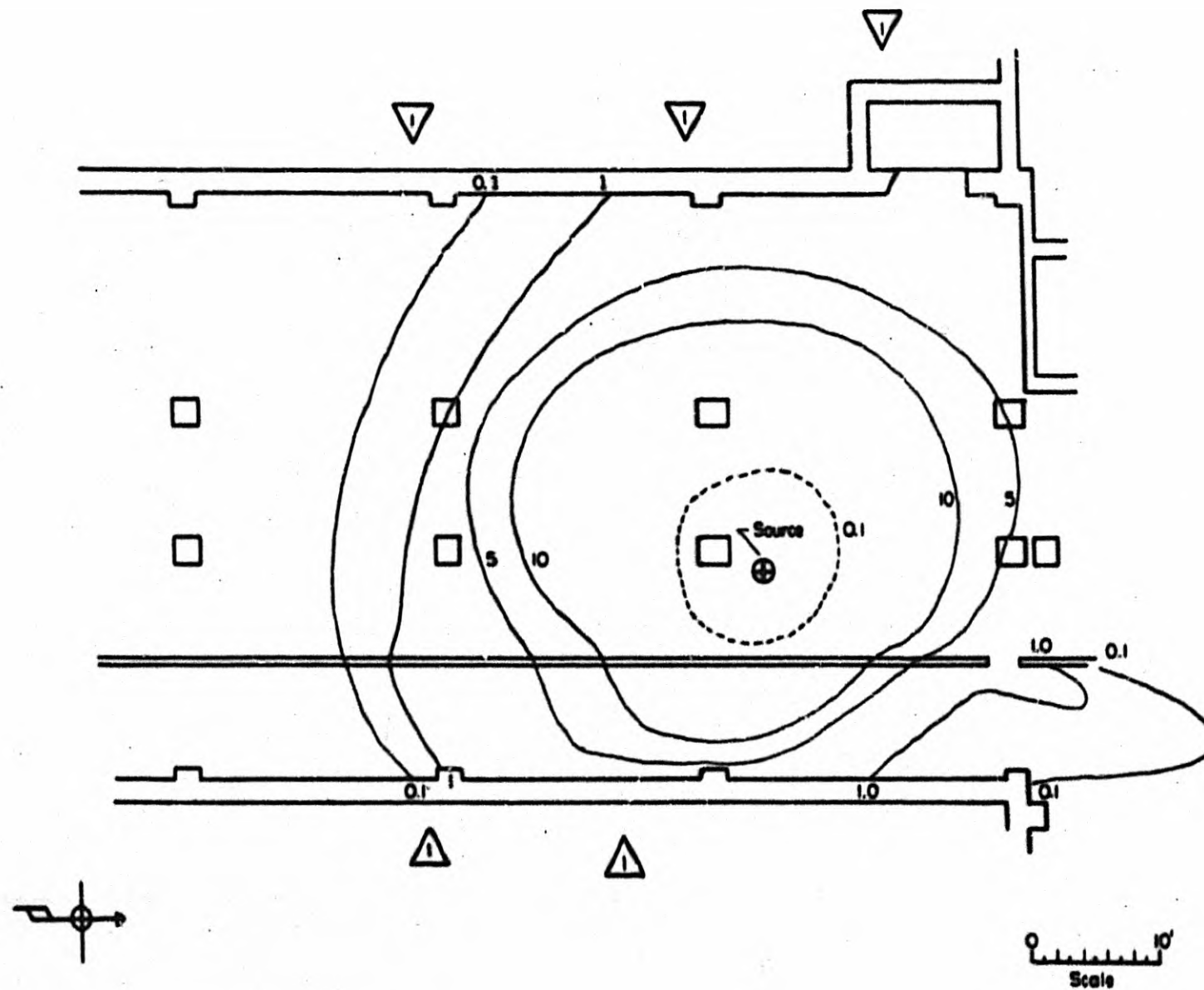


Fig. 3.12--Point source below air filter in wing D. —, Basement values, mr/hr/curie . - - -, First-floor values, mr/hr/curie . ▽, Locations of office partitions running perpendicular to external walls on the first floor.

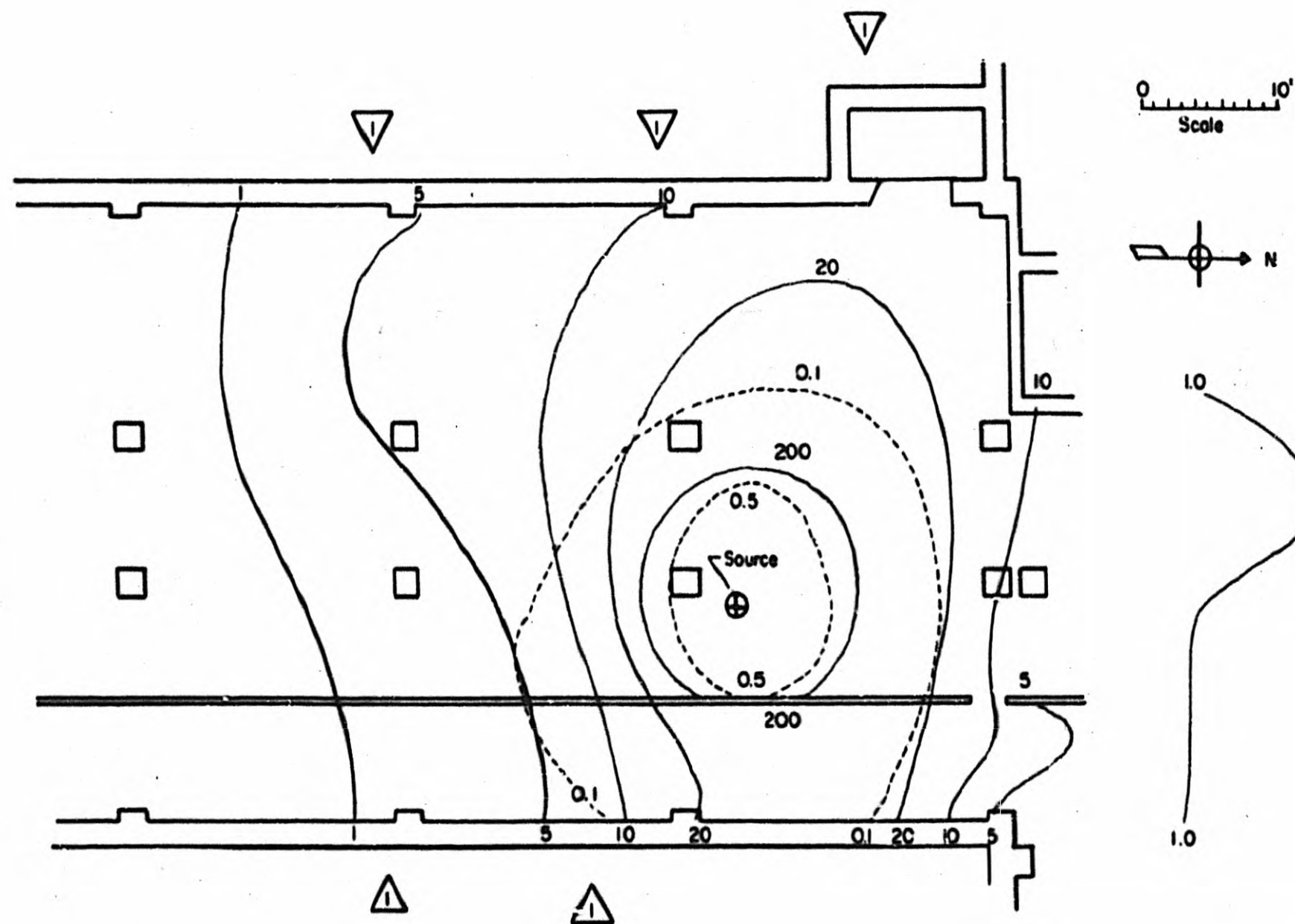


Fig. 3.13—Point source above air filter in wing D. —, Basement values, mr/hr/curie. - - -, First-floor values, mr/hr/curie. ▽, Locations of office partitions running perpendicular to external walls on the first floor.

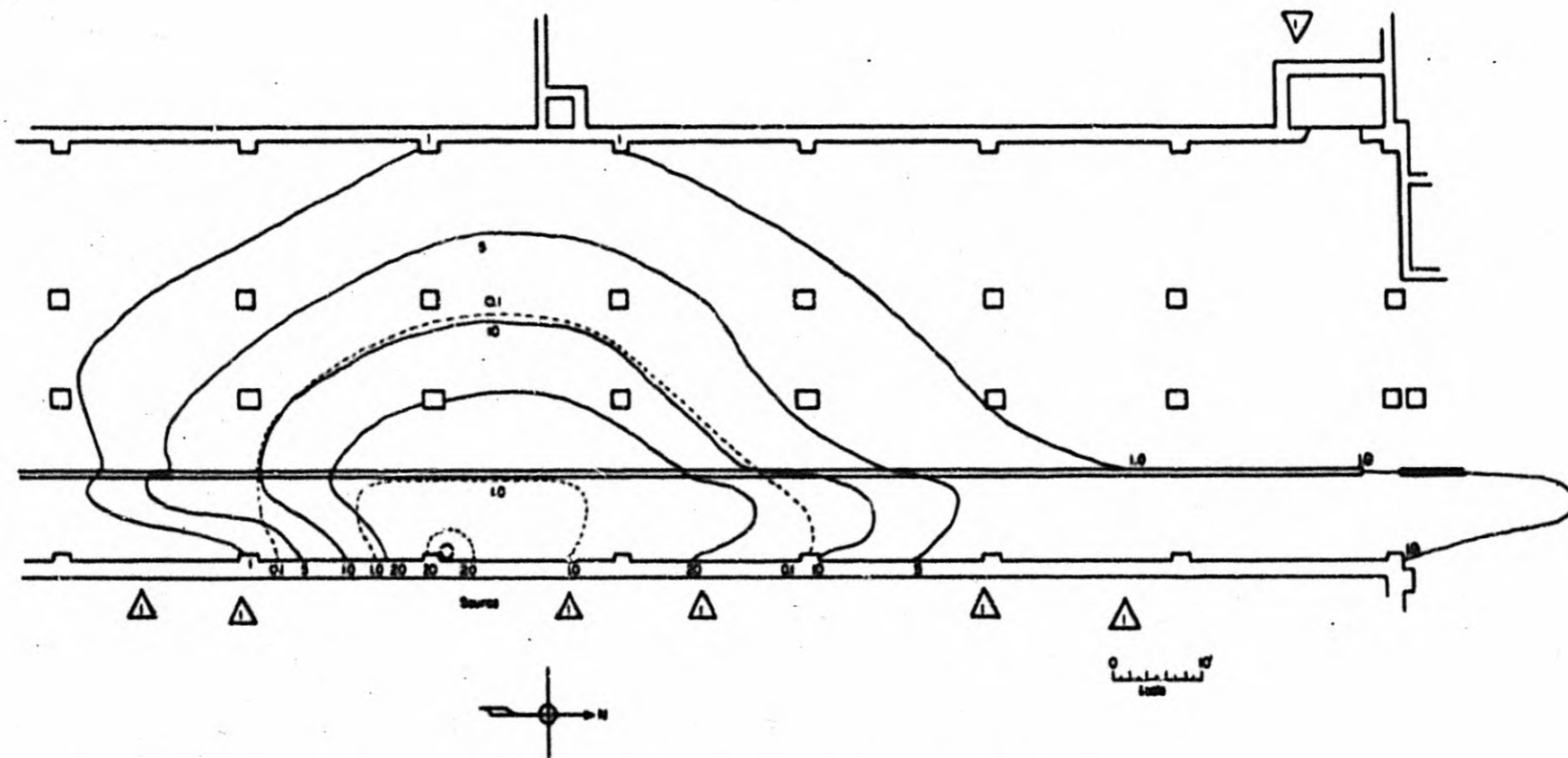


Fig. 3.14—Point source below roof drain in wing D. —, Basement values, mr/hr/curie. - - -, First-floor values, mr/hr/curie. ▽, Locations of office partitions running perpendicular to external walls on the first floor.

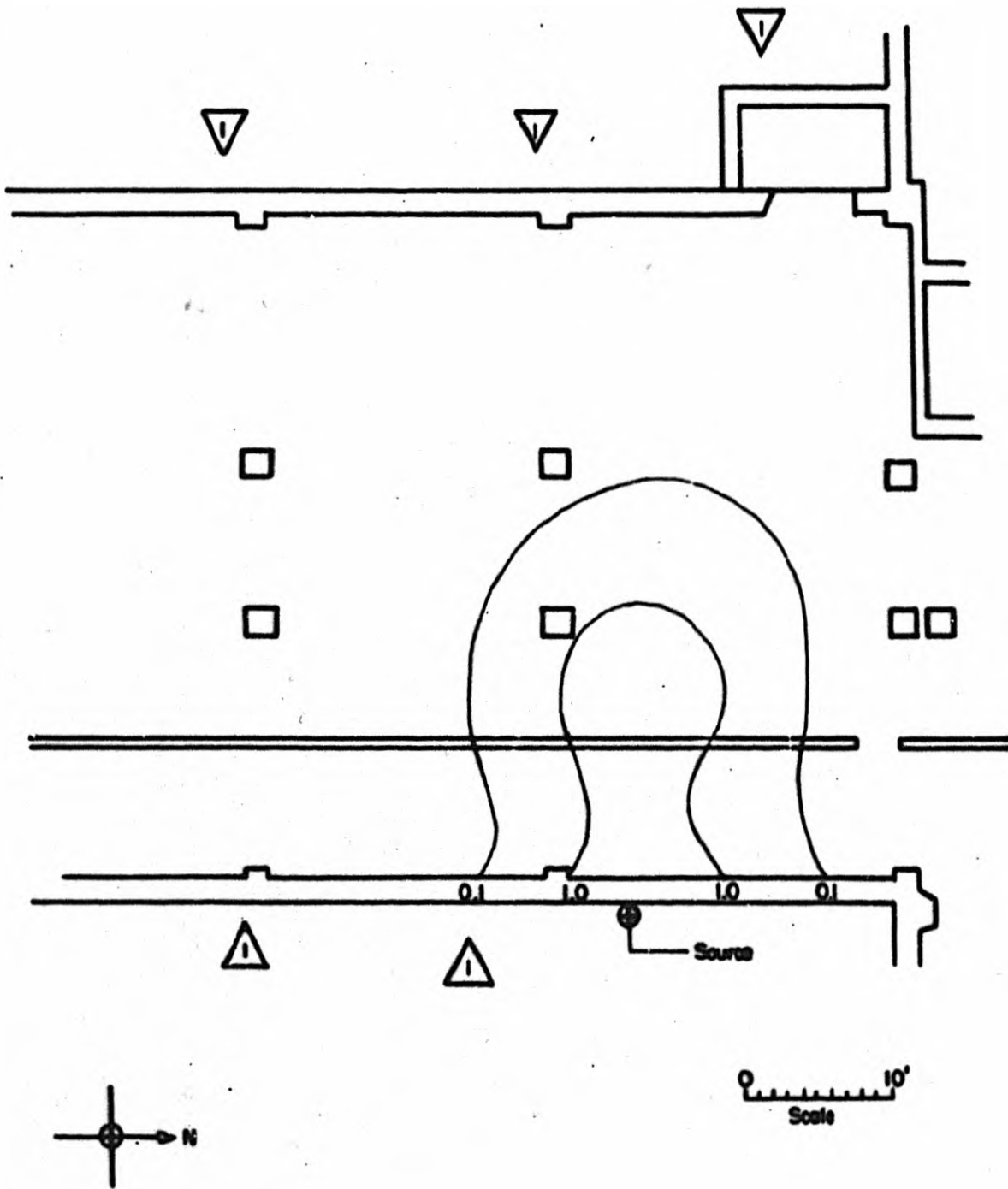


Fig. 3.15—Point source in emergency air inlet in wing D. —, Basement values, mr/hr/curie. ▽, Locations of office partitions running perpendicular to external walls on the first floor.

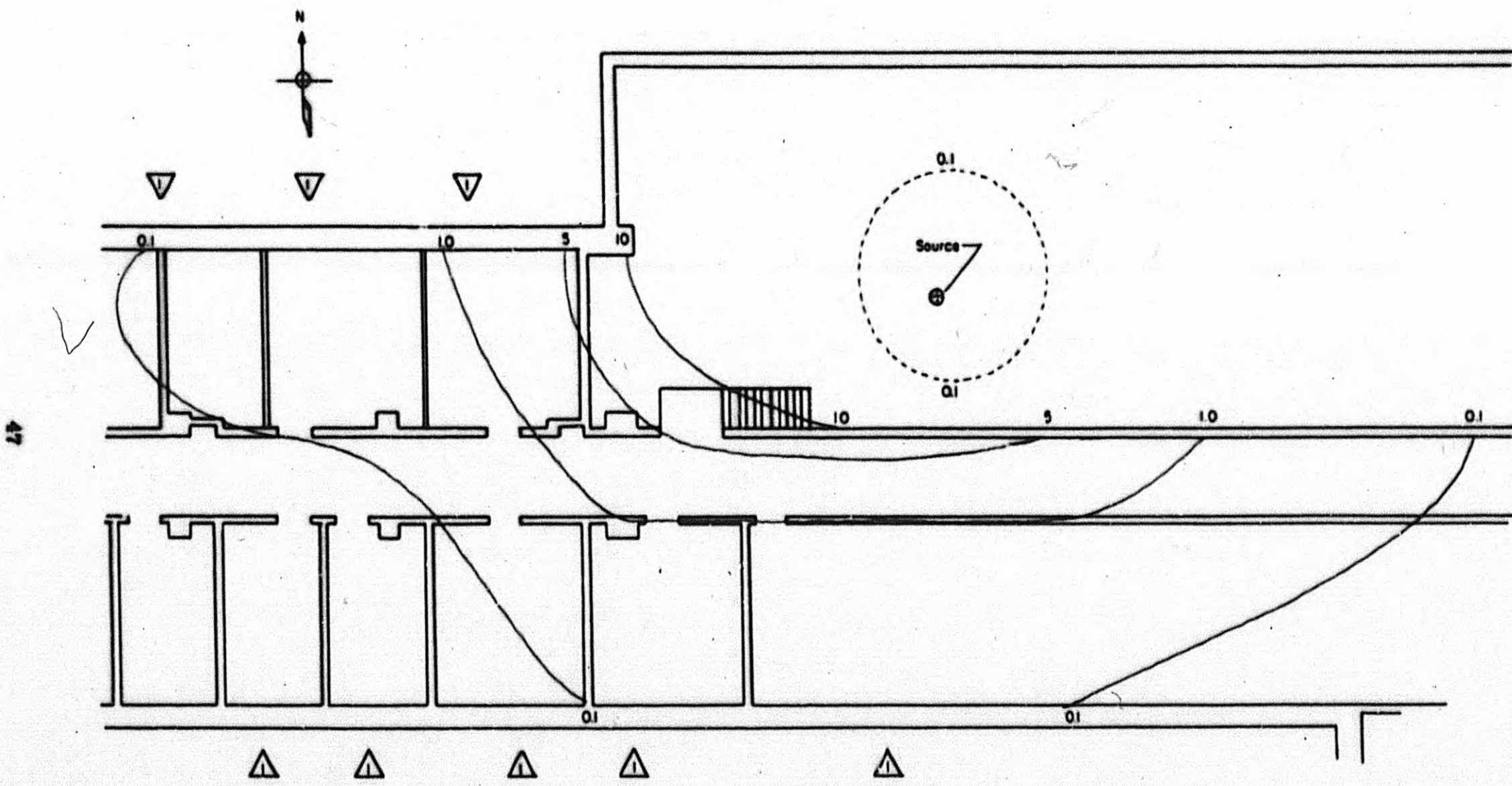


Fig. 3.16—Point source below air filter in wing A. —, Basement values, mr/hr/curie. - - -, First-floor values, mr/hr/curie. ▽, Locations of office partitions running perpendicular to external walls on the first floor.

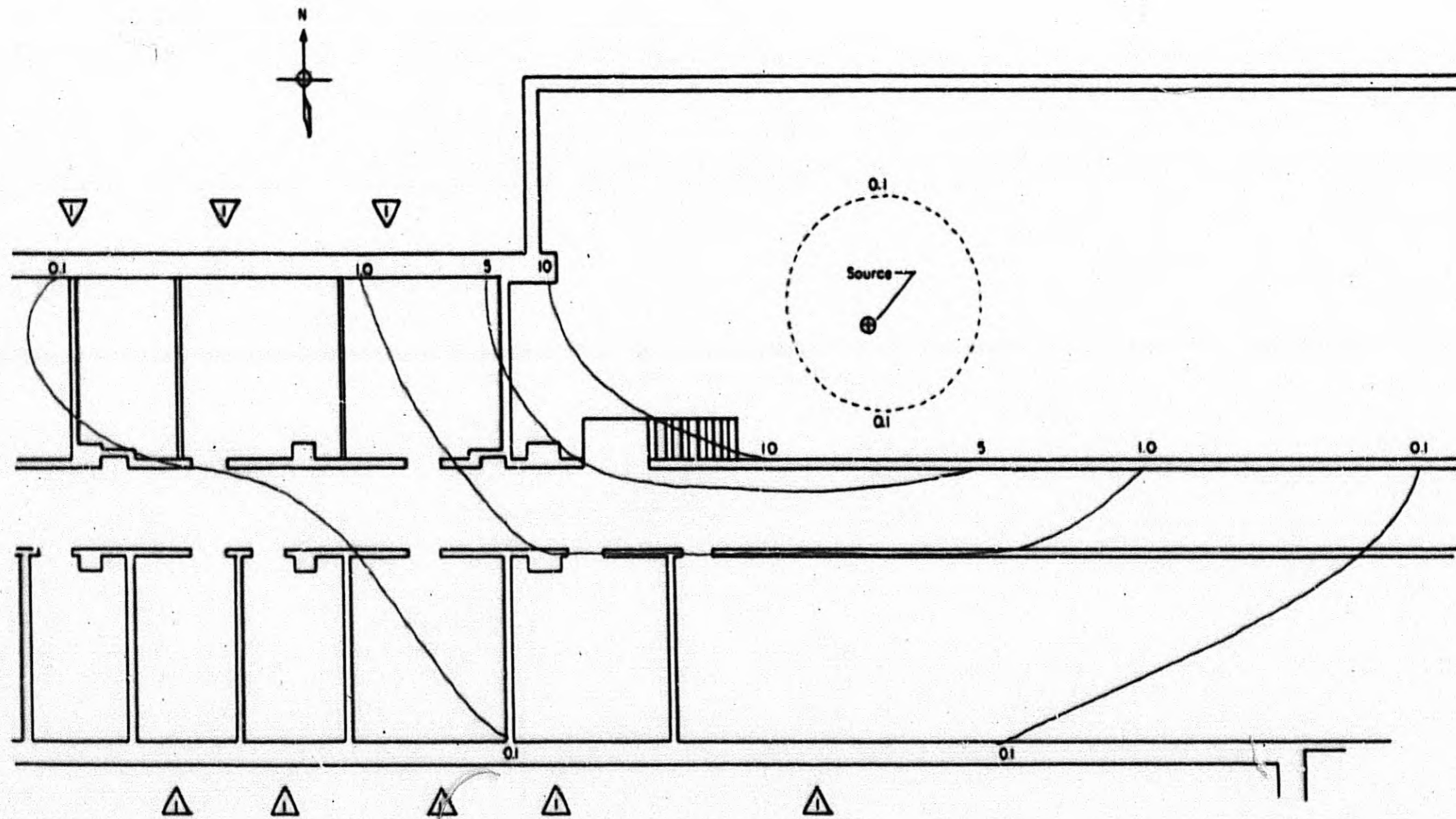


Fig. 3.17—Point source above air filter in wing A. —, Basement values, mr/hr/curie . - - -, First-floor values, mr/hr/curie . ▽, Locations of office partitions running perpendicular to external walls on the first floor.

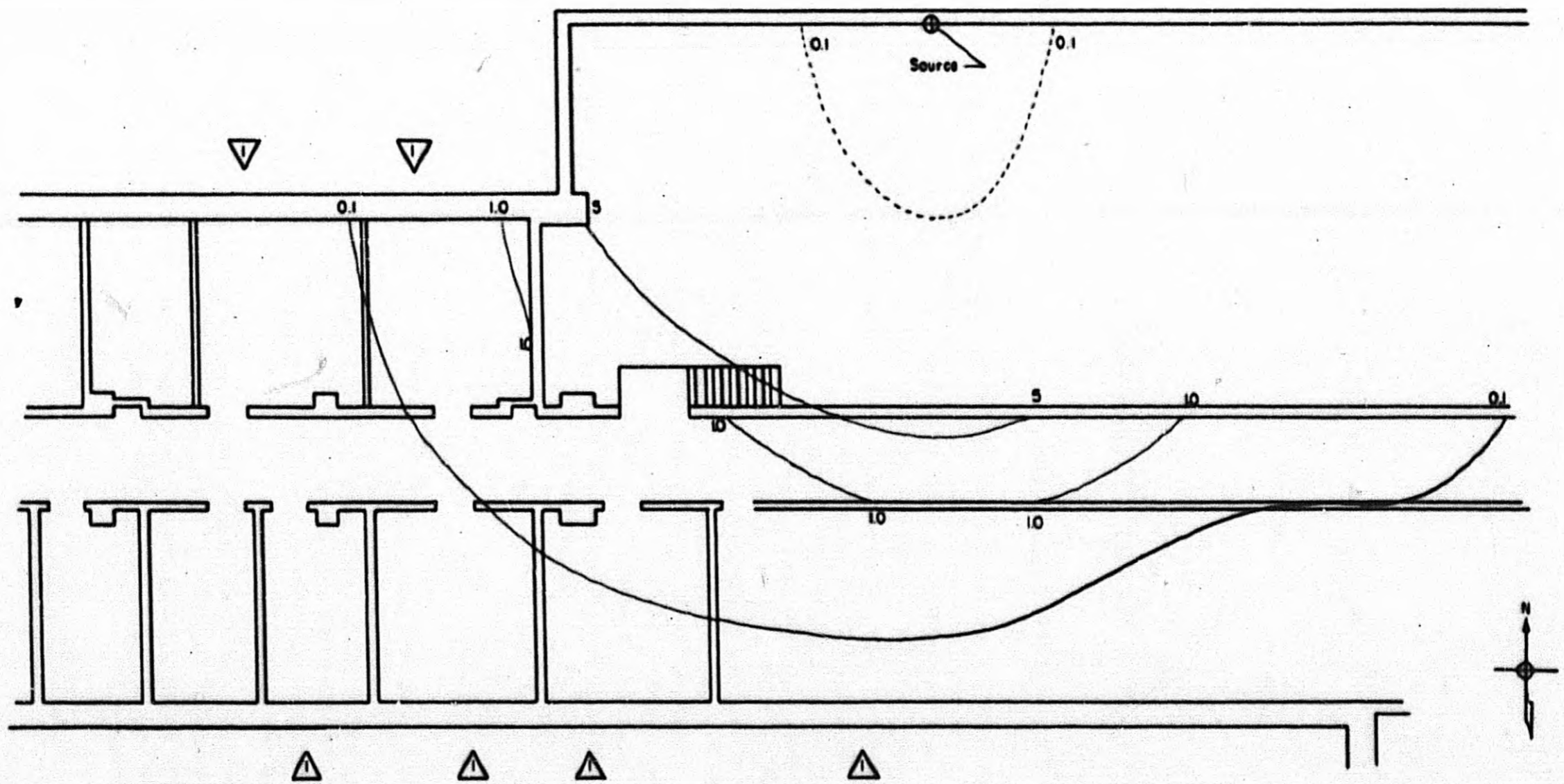


Fig. 3.18—Point source in emergency air inlet in wing A. —, Basement values, mr/hr/curie. - - -, First-floor values, mr/hr/curie.
 ▽, Locations of office partitions running perpendicular to external walls on the first floor.

Chapter 4

ANALYSIS AND CONCLUSIONS

4.1 ESTIMATION OF INFINITE-FIELD DOSE

Although experimental simulation of a radiation field may be carried out to large distances from the structure to be measured, it is obvious that the extension of the field much beyond one mean free path requires extremely strong sources if adequate measurements are to be made. This is both impractical and uneconomical. However, an estimation of the contribution that would be obtained from the remaining area not covered by the simulated source must be made if protection factors are to be calculated.

Therefore the experiments were planned in such a way as to minimize, as much as possible, the error that might be introduced by such an estimation. Experimental source distributions were laid out in concentric annular areas so that comparison between experiment and theory could most readily be made. Dose rates contributed by each annulus could be calculated in terms of the infinite-field dose rate and compared with the experimental results; the best fit among the various rings would thus yield the infinite-field dose rate. Also, the experimental field was laid out whenever possible to such a distance that the additional contribution from the uncovered area would be relatively small.

The following analysis was used to obtain ratios of annular to infinite-field dose rates. If air scattering and absorption are neglected, the dose contribution^{1,2} from an annular area dA to a point P can be written as

$$dR_d = \frac{q\sigma 2\pi r dr}{\sqrt{(r^2 + h^2 + x_1^2) - 4r^2x_1^2}} \quad (4.1)$$

where R_d = dose rate from direct radiation

σ = density of contamination per unit area

q = dose rate at a unit distance from a 1-curie source

r = radius of differential annular area

h = height above plane where measurement is desired

x_1 = eccentricity of detector

The denominator of this equation represents the square of the geometric mean distance between a detector located at P and the closest and farthest points on the source annulus. Therefore the square root of this quantity can be taken as the mean attenuation distance. Thus the direct dose contribution, taking into account the absorption coefficient of air, from an annular area can be approximated as

$$dR_d = \frac{2\pi\sigma q r dr \exp -\mu [(r^2 + h^2 + x_1^2) - 4r^2x_1^2]^{1/2}}{\sqrt{(r^2 + h^2 + x_1^2) - 4r^2x_1^2}} \quad (4.2)$$

where $x_1 \ll r$ and μ is the total absorption coefficient of air. Thus, integrating, the direct dose to a point P within a cleared circle of radius a in an infinite contaminated field can be written as

$$R_d = 2\pi\sigma q \int_{Y_a}^{\infty} \frac{e^{-\mu y}}{y} dy = 2\pi\sigma q E_1(\mu Y_a) \quad (4.3)$$

where

$$Y_a = [(a^2 + h^2 + x_1^2)^2 - 4a^2x_1^2]^{1/4}$$

and E_1 is the well-known exponential integral of order 1. To this, however, must be added the contribution from air-scattered radiation. The total radiation, direct and scattered, received by a detector can be expressed as the direct contribution times a build-up factor B. One useful expression for this build-up factor is

$$B(\mu y) = 1 + k\mu y \quad (4.4)$$

where k is constant over the range of interest. Experiments performed at Brookhaven National Laboratory have indicated a value of $k = 0.55$ from cobalt radiation near a ground-air interface.³

By analogy with Eq. 4.3, the scattered contribution can be directly written as

$$R_s = 2\pi\sigma q \int_{Y_1}^{\infty} h\mu e^{-\mu y} dy \quad (4.5)$$

Thus the ratio of the total far-field radiation extending beyond radius b (see Fig. 4.1) to an annular radiation field extending from radius a to b can be set forth as

$$\text{Ratio} = \frac{E_1(\mu Y_b) + 0.55(e^{-\mu Y_b})}{E_1(\mu Y_a) - E_1(\mu Y_b) + 0.55(e^{-\mu Y_a} - e^{-\mu Y_b})} \quad (4.6)$$

where

$$Y_a = [(a^2 + h^2 + x_1^2)^2 - 4a^2x_1^2]^{1/4}$$

and

$$Y_b = [(b^2 + h^2 + x_1^2)^2 - 4b^2x_1^2]^{1/4}$$

4.2 CALCULATION OF PROTECTION FACTORS

The following procedure was used to calculate the protection factor provided by any location within the building. First, the experimental data obtained were normalized to the source density required to create a radiation field of 1 r/hr at 1 meter above an infinite source field. The normalized data from the source annulus lying farthest from the point of interest were then multiplied by the ratio (Eq. 4.6) to estimate the infinite-field contribution. This infinite-field contribution was then adjusted to provide for the fact that certain wings were shielded from some of the far-field direct (but not scattered) radiation by other portions of the structure.

Thus the total radiation received at any point is composed of three parts: (1) the radiation from sources on the building roof (experimentally measured); (2) the radiation from close-in sources on the ground (experimentally measured); and (3) the radiation from the infinite field extending beyond the simulated ground sources (analytically estimated). It should be noted that the estimated far-out radiation sources, in general, contributed less than 30 per cent of the total radiation received by the building. The protection factor (P.F.) is then deter-

mined by dividing the infinite-field value of 1000 mr/hr by the sum of the normalized experimental and estimated contributions. Thus

$$P.F. = \frac{1000}{\text{roof contribution} + \text{ground contribution}}$$

Since the building was, in general, composed of wings of identical construction, the argument of similarity was used where applicable to predict the dose rates where no experimental measurements were made.

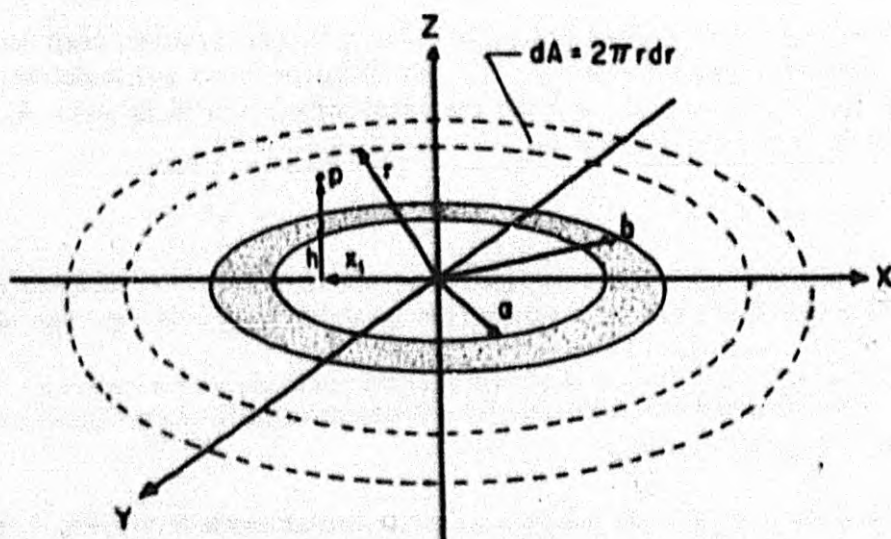


Fig. 4.1 — Diagram of contaminated plane with cleared circle.

As an example of this procedure, consider the computation of the protection factor of point 5 on the third floor of wing F. As shown in Table 4.1, the raw experimental data are divided by the exposure time and the source density and multiplied by the standard source density,* 0.062 megacurie per square mile, to obtain the normalized experimental dose rates.

By substitution into Eq. 4.6,

$$\mu = 2.3 \times 10^{-3} \text{ ft}; \quad b = 152 \text{ ft}; \quad a = 80 \text{ ft}; \quad h = 35 \text{ ft}; \quad x_1 = 21\frac{1}{2} \text{ ft}$$

The ratio of the far-field dose to the dose produced from contamination within the annular area lying between 80 to 152 ft radii is found to be 2.4; multiplying this by the average value of the dose rate experimentally measured from this area provides an estimate of the dose rate that would arise from contamination lying beyond the 152-ft radius. The value for the far-field dose in this case is 1.3 mr/hr.

The protection factor of this location can now be calculated by the use of average values from Table 4.1:

$$P.F. = \frac{1000}{(0.14) + 2(0.26 + 0.51 + 1.20)} = 245$$

The factor of 2 appearing in the denominator is needed because the source was exposed around only one-half of the building (i.e., symmetry was used). Finally, rounding off to the nearest 10 gives a protection factor (at location 5 on the third floor of wing F) of 250.

Figures 4.2 to 4.4 present the protection factors calculated for wing A, wings B and C, and wings F and G, respectively, in tabular form, along with a plot plan of the structure which indicates their positions. The protection factor afforded by any other location within the build-

* An infinite flat plane contaminated with 0.062 megacurie of Co^{60} per square mile would produce a 1 r/hr dose rate at 1 meter.

ing may be inferred by comparison with a similar location in one of the wings shown in these drawings.

4.3 "NEAR WINDOW" EFFECT

The analysis of the protection afforded by this structure is of necessity based upon average conditions. It was therefore important to investigate the effect of localized high-radiation areas caused by apertures, such as windows and doors, in external walls. Figure 4.5 presents the results of a series of experiments that were conducted on the northwest side of wing A (see Fig. 3.1) to determine this effect. The following general conclusions can be drawn from these data.

1. Beyond distances of approximately 8 ft from the inner face of the external wall, radiation fields are nearly uniform along the length of the building.
2. At the inner face of the external walls, the dose rate is approximately a factor of 5 lower than at a similar position behind a window.
3. An additional protection factor of at least 2 may be gained below the window sill levels.

These conclusions were drawn from data taken on the first floor and therefore apply only to that level. However, indirect evidence indicates that similar conclusions may be made concerning the upper floors, with the exception of the top floor where roof sources alter the gen-

TABLE 4.1—DATA NORMALIZATION

Radiation field	Position	Experimental dose, mr	Exposure time	Source density, megacuries/square mile	Normalized experimental dose rate,* mr/hr
Roof	F-30	10.9	9 hr, 5 min	0.57	0.13
	F-31	12.9			0.16
	F-32	10.9			0.13
	F-33	13.1			0.16
0 to 80 ft	F-30	14.9	8 hr, 14 min	0.57	0.20
	F-31	22.3			0.30
	F-32	19.8			0.27
	F-33	19.1			0.26
80 to 152 ft	F-30	17.4	6 hr, 42 min	0.28	0.58
	F-31	15.6			0.52
	F-32	14.1			0.47
	F-33	14.4			0.48

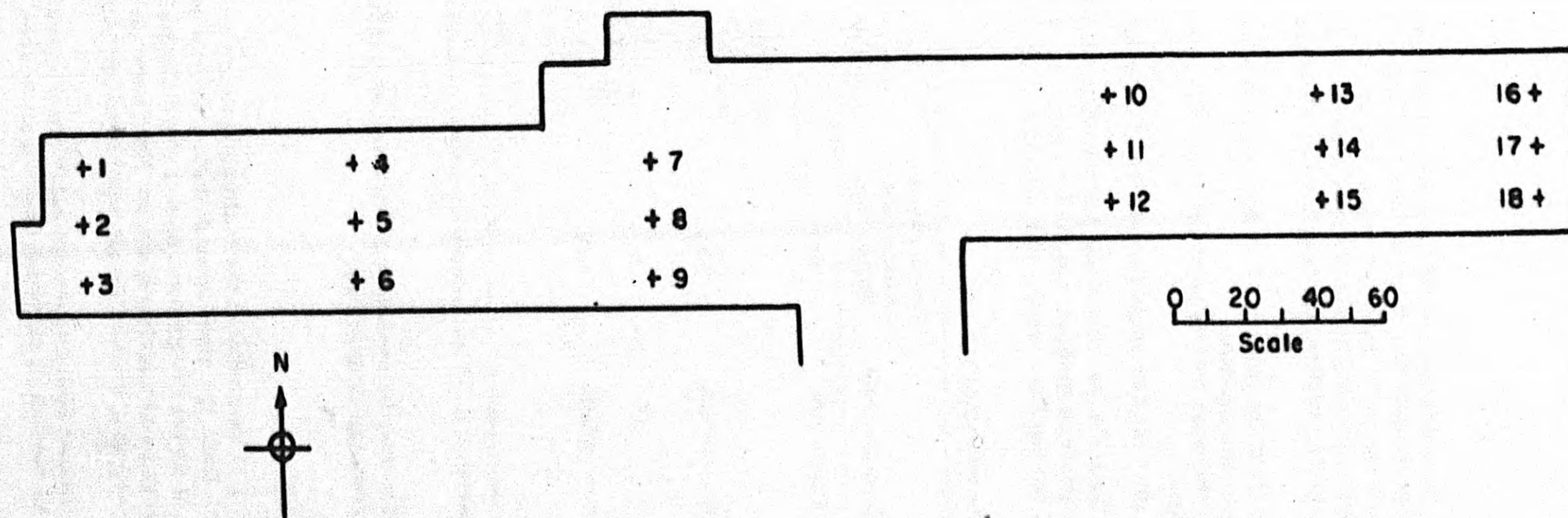
* An infinite flat plane contaminated with 0.062 megacurie of Co^{60} per square mile would produce a 1 r/hr dose rate at 1 meter.

eral pattern of radiation. In general, the situation may be considered characteristic of buildings with heavy floors and walls with a high percentage of openings.

4.4 EFFECT OF EXPOSED BASEMENT WALLS

The rolling contour of the ground (see Fig. 1.1) surrounding the building caused varying percentages of the basement wall to be exposed. Since the experimental measurements were performed on different sections of the building, a direct comparison of this effect on the shelter factor could be measured. Such comparisons were particularly significant here because of the relatively great thickness of the first floor, providing considerable attenuation to radiation entering the building above it.

Figure 4.6 presents the experimentally measured effectiveness of earth covering various proportions of the basement wall. In general, the measured radiation doses may be seen to be



Position	1	2	3	4	5	6	7	8	9	10	11	12	13	14	15	16	17	18
Basement	400	910	710	1800	2300	1900	1900	2300	2000	1900	2300	2000	1800	2300	1900	400	910	400
First Floor	30	100	50	30	80	40	30	90	40	30	90	40	30	80	40	30	80	40
Second Floor	60	260	90	50	220	70	100	400	140	100	400	140	50	220	70	60	200	60
Third Floor	70	260	130	70	270	130	110	440	220	80	320	160	70	270	140	70	230	70
Fourth Floor	80	100	90	80	100	80	90	120	100	60	70	60	60	70	60	80	90	80

Fig. 4.2—Protection factors from Co^{60} radiation in wing A.

Position	1	2	3	4	5	6	7	8	9	10	11	12	13	14	15	16	17	18
Basement	1500	2500	1500	1700	2500	1700	1700	2500	1700	2000	2400	2000	2000	2400	2000	900	940	980
First Floor	50	100	50	20	80	20	40	120	40	500	1000	300	50	120	50	20	70	20
Second Floor	100	410	100	60	240	60	70	200	70	1000	1500	1000	250	740	250	290	320	290
Third Floor	110	400	110	70	260	70	90	240	90	870	1200	900	240	440	240	470	540	470
Fourth Floor	60	120	60	50	110	50	60	120	60	120	150	120	100	130	100	80	110	80

8

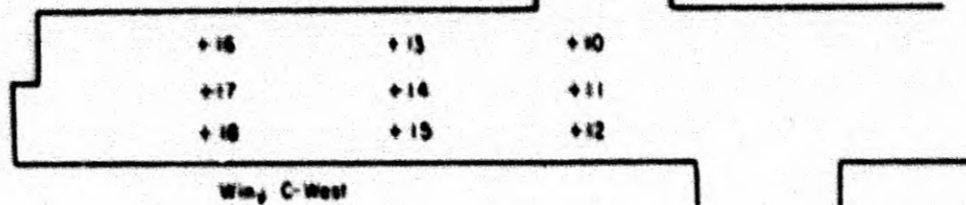
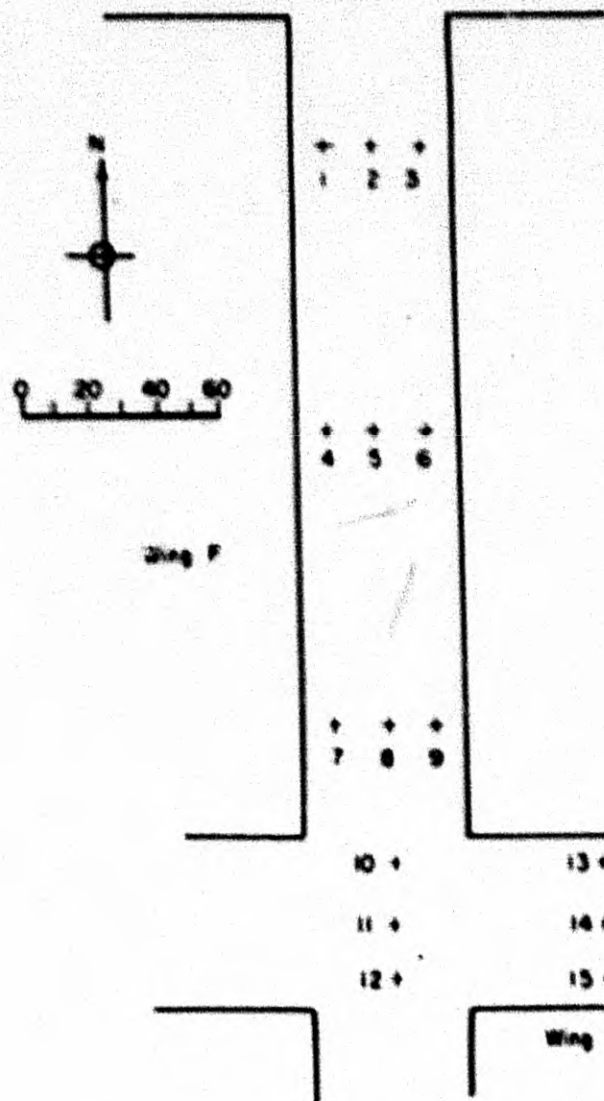


Fig. 4.3—Protection factors from Co^{60} radiation in wing B and wing C west.



Position	1	2	3	4	5	6	7	8	9	10	11	12	13	14	15	16	17	18	19
Basement	20,000																		
First Floor	50	60	60	30	40	30	30	50	30	500	1000	500	30	60	30	30	60	30	30
Second Floor	60	200	60	30	200	30	60	120	60	1000	1500	1000	70	120	60	200	200	60	60
Third Floor	120	400	120	30	250	30	100	300	100	600	1200	600	100	270	70	70	220	70	70
Fourth Floor	60	120	60	60	120	70	60	120	60	120	120	120	60	70	60	60	60	60	60

Fig. 4.4—Protection factors from Co⁶⁰ radiation in wing F and wing G east.

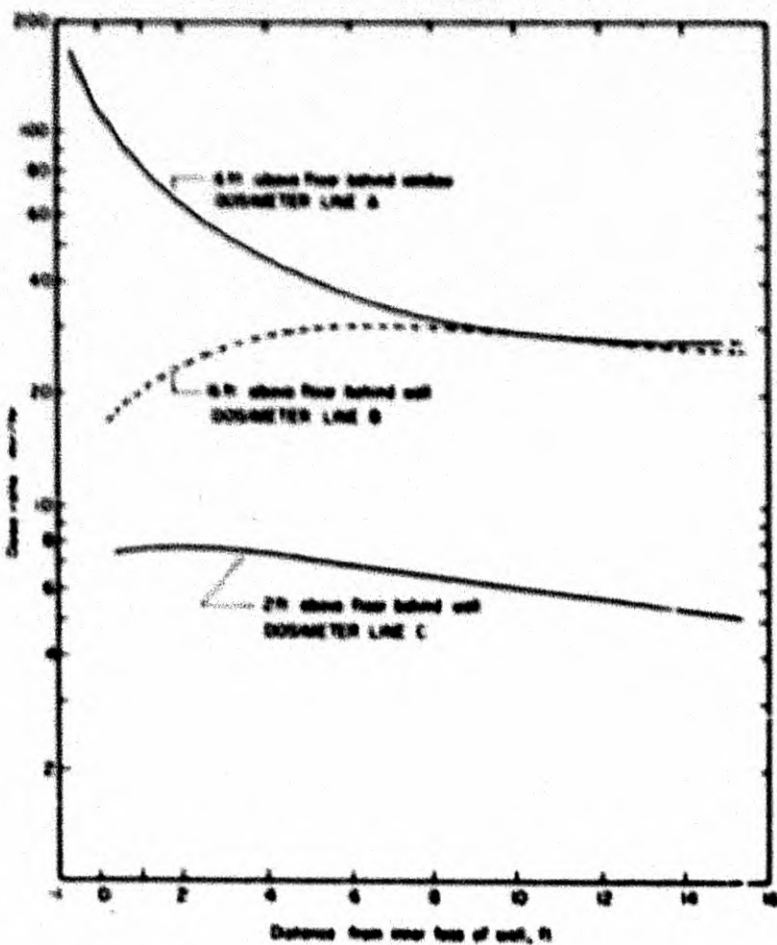
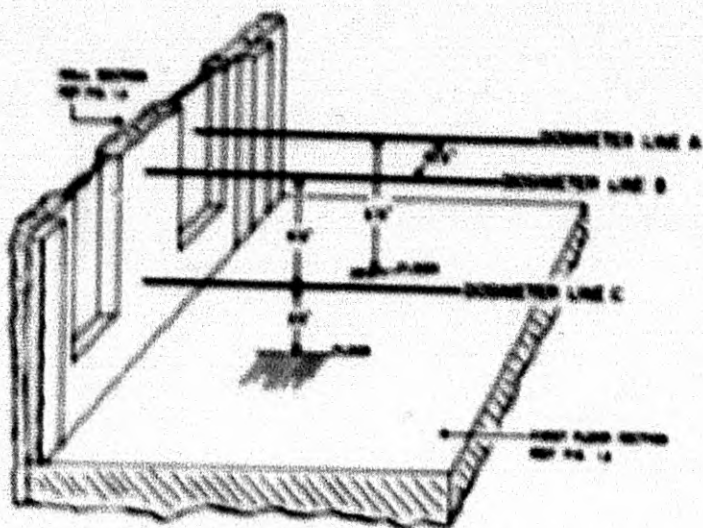


Fig. 4.3—Horizontal dose distribution on the first floor from a semicircular radiation field of 200 ft radius.

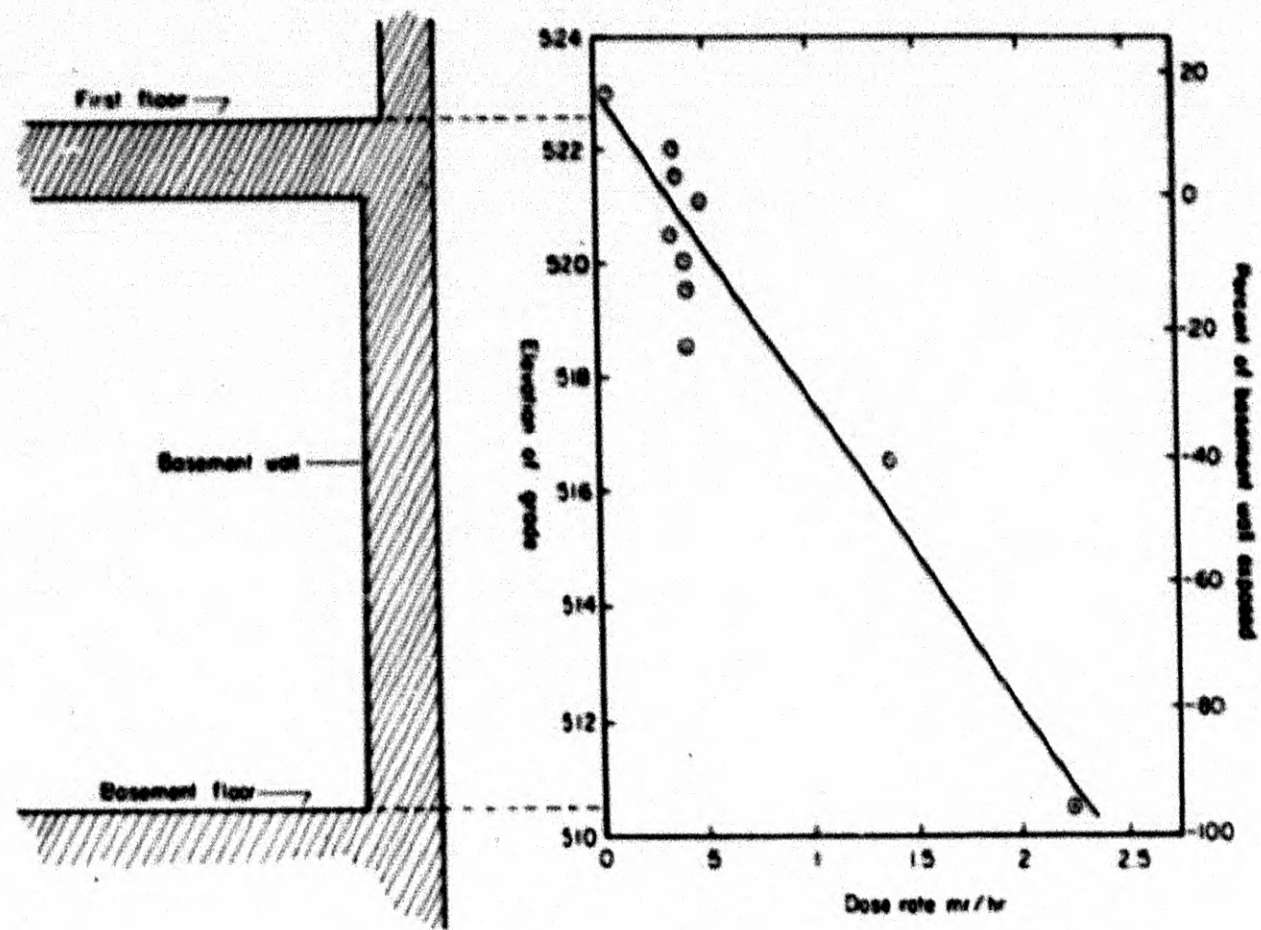


Fig. 4.1— Effect of exposed basement wall.

approximately proportional to the amount of basement wall exposed. Both experimental and analytical methods indicate that by burying the basement wall below grade (i.e., grading the land above the elevation of the first floor) a significant reduction in radiation penetration may be achieved since the only significant path remaining for radiation entrance to the basement is scattering from the structure or atmosphere above and penetration through the thick floor slab.

4.5 GENERAL CONCLUSIONS

In many instances, general conclusions, applying to a large portion of the building, can be made from the analysis and data presented. These are as follows:

1. As was expected, the shelter factor is highest in the basement of the structure where the walls are not exposed above ground. The shelter factors found typical are:

Location (center corridor)	Factor
Basement	500* to 10,000
First floor	80 to 100
Second floor	200 to 300
Third floor	250, 250†
Fourth floor	100, 50†

2. Complete burial of the basement wall so that the land is graded above the elevation of the first floor significantly reduces radiation penetration.

3. Average conditions (i.e., the radiation field is fairly uniform in longitudinal building direction) exist beyond distances of approximately 8 ft from the inner face of an external wall.

4. The dose rate is 5 to 10 times higher than average at the immediate inside of a window opening.

5. An additional protection factor of at least 2 may be gained on the first floor below window sill level.

6. The effect of concentrated fallout located within the shelter area in air filters and roof drains may be disastrous to shelter capability. A shelter factor of less than 1 (dose rate in shelter higher than that outside shelter) is possible in an appreciable portion of the basement if a large amount of fallout material is concentrated in the emergency air filters situated within the shelter area.

7. As a result of the measurements with a source located in the initial air plenum chamber (see Figs. 3.10, 3.15, and 3.18), it seems that emergency air filters could be reinstalled profitably in this location outside the blastproof portion of the basement if fallout accumulations in the filter were expected to be great.

REFERENCES

1. J. A. Auxier et al., Experimental Evaluation of the Radiation Protection Afforded by Residential Structures Against Distributed Sources, Report CEX-58.1, Jan. 19, 1959.
2. G. J. Hine and G. L. Brownell, "Radiation Dosimetry," p. 762, Academic Press, Inc., New York, 1956.
3. L. R. Solon, Keran O'Brien, and Hugo Di Giovanni, Measurement of the Scatter Component from a Kilocurie Cobalt-60 Source, Report NYO-2065, June 10, 1957.

* Near totally exposed basement wall (no windows).

† Nontypical thin roof exists in wing A east only.

Appendix A

RADIATION-SAFETY OPERATIONS

By

James E. Turner

Health Protection Branch
Division of Biology and Medicine
U. S. Atomic Energy Commission

This appendix describes the radiation-safety plan used during the survey of the AEC Headquarters building. None of the 1800 employees having the normal 8:30 a.m. to 5:00 p.m. working hours were exposed to the sources because all measurements were made during off hours and on week ends. The survey was successfully completed with a minimum of disruption to employees who were on duty when the sources were being used. There were no unusual incidents, and the experimental measurements were safely made within the criteria established by this plan for radiation-safety operations.

Radiation-safety monitoring during the survey was divided into two operations:

1. Safety of personnel handling the sources and performing the experiments.
2. Safety of persons present in the building and on the grounds but not involved in making the survey. (Off-site radiation levels were at background most of the time and never exceeded about 1.5 mr/hr in extreme cases.)

The first of these two operations was the responsibility of the contractor performing the survey (TOI). This Appendix outlines some of the measures taken with respect to the second operation.

Although the survey was restricted to the nonworking hours of the AEC office staff, a considerable number of employees (engineers, guards, telephone operators, cleaning crews, etc.) were present on the building site on a 24-hr basis. Minimizing radiation exposure of these persons was complicated by the fact that the building had no special facilities for handling radioactive sources or for setting up restricted radiation zones. In addition, few of the employees on duty, if any, had had experience working in the vicinity of radiation sources. As described in the text, areas into which there was normally access might have high radiation levels at times. Extreme care had to be exercised in securing all conceivable entrances to a radiation zone prior to starting a run. These factors contributed to making the radiological-safety operation somewhat unusual and difficult.

In this regard a detailed radiological-safety plan was drawn up by the staff of the AEC Division of Biology and Medicine (DBM) prior to the beginning of the building survey. It was decided that the radiological safety of building employees would be the responsibility of DBM and would be carried out by members of the staff trained in this field; DBM would also furnish radiation-monitoring instruments for the survey from its instrument shop.

During each set of measurements made by TOI, there were three members of the DBM staff present. They were designated, respectively, as the DBM Representative, the Radiologi-

cal-Safety (Rad-Safe) Officer, and the Radiation-Instruments (Rad-Inst) Officer. Procedures to be carried out by the Rad-Safe Officer, assisted by the Rad-Inst Officer, in connection with every run were set forth in the form of a check list (see below). In general, the radiological-safety plan gave responsibility to the Rad-Safe Officer for seeing (1) that persons not involved in the experiments or operations connected with them would not be exposed to a dose of more than 30 mr from one day's operations, unless approved by the DBM Representative, and (2) that all persons who might be expected to receive a dose of more than 30 mr wear film badges.

Advance notification of all runs was sent in writing to the entire AEC staff. Immediately before each run the three members of DBM on duty decided which areas of the building and grounds would be restricted as radiation zones during the run. Barricades and signs were then erected. Signs on the barricades gave information about alternate entrance routes into the building and instructions about who should be contacted if entrance to the restricted area were necessary. In addition, doors and elevators were locked, and appropriate signs were posted where feasible. Before actual start-up a series of telephone calls was made to guard, maintenance, and clean-up shift supervisors to make certain their crews were advised of the restricted areas and the approximate duration of the run. Before the source was released, a final visual inspection was made to ensure that no unauthorized persons were present in the restricted areas. After these precautionary checks the DBM Representative authorized the initiation of the run. During the run the Rad-Safe and Rad-Inst Officers made surveys of the radiation zone and recorded readings in a log. The Rad-Inst Officer patrolled areas outside the building in a truck and kept the area where the source was located under surveillance. He maintained contact with guard headquarters in the building by two-way radio. The DBM Representative was notified at the conclusion of the run. The Rad-Safe Officer notified the guard force and shift supervisors, and the barricades were removed.

The check list for the operation included the following items:

A. Before Operation

1. Determine restricted areas and place radiation signs and instructions at appropriate locations in the building.
2. Place outside road blocks as needed, with warning signs and instructions as to alternate entrance routes onto the site.
3. Inform shift supervisors of the run and give them a brief description of the operation.
4. Issue film badges and pocket chambers to appropriate personnel.
5. See that X-ray film or other materials that could be damaged by radiation from the run will not be exposed.

B. During Operation

1. Take occasional readings and make checks in the restricted areas to see that they are clear of unauthorized personnel.
2. Maintain regular contact with the truck patrolling outside the building.
3. Oversee any operations that may involve exposures of personnel to radiation levels in excess of about 100 mr/hr.
4. Keep log of activities.
5. Be prepared for radiological emergencies. (Locations of first-aid kits and telephone numbers of DBM physicians were given in the check list.)

C. After Operation

1. Measure background and confirm that source has been secured in its container.
2. Notify shift supervisors that run is over. Inform them of any changes in the restricted areas for the next operation.
3. Collect film badges and pocket chambers.
4. Read pocket chambers and record readings in log.
5. Remove or relocate signs and barriers as appropriate.
6. Confirm staffing and start-up time of next operation.